Morphodynamics of boulder-bed semi-alluvial streams in northern Fennoscandia: a flume experiment to determine sediment self-organization

Lina E. Polvi[1,1]

[1]Umeå University

November 30, 2022

Abstract

In northern Fennoscandia, semi-alluvial boulder-bed channels with coarse glacial legacy sediment are abundant, and due to widespread anthropogenic manipulation during timber-floating, unimpacted reference reaches are rare. The landscape context of these semi-alluvial rapids— with numerous mainstem lakes that buffer high flows and sediment connectivity in addition to a regional low sediment yield— contribute to low amounts of fine sediment and incompetent flows to transport boulders. To determine the morphodynamics of semi-alluvial rapids and potential self-organization of sediment with multiple high flows, a flume experiment was designed and carried out to mimic conditions in semi-alluvial rapids in northern Fennoscandia. Two slope setups (2% and 5%) were used to model a range of flows (Q1 (summer high flow), Q2, Q10 & Q50) in a 8 x 1.1 m flume with a sediment distribution analogous to field conditions; bed topography was measured using structure-from-motion photogrammetry after each flow to obtain DEMs. No classic steep coarse-bed channel bedforms (e.g., step-pools) developed. However, similarly to boulder-bed channels with low relative submergence, at Q10 and Q50 flows, sediment deposited upstream of boulders and scoured downstream. Because the Q50 flow was not able to re-work the channel by disrupting grain-interlocking from preceding lower flows, transporting boulders, or forming channel-spanning boulders, the channel-forming discharge is larger than the Q50. These results have implications for restoration of gravel spawning beds in northern Fennoscandia and highlight the importance of large grains in understanding channel morphodynamics.

Hosted file

essoar.10504441.2.docx available at https://authorea.com/users/474987/articles/608906-morphodynamics-of-boulder-bed-semi-alluvial-streams-in-northern-fennoscandia-a-flume-experiment-to-determine-sediment-self-organization

Morphodynamics of boulder-bed semi-alluvial streams in northern Fennoscandia: a flume experiment to determine sediment self-organization

L. E. Polvi[1]

[1]Department of Ecology & Environmental Science, Umeå University, Umeå, 907 36 Sweden

Corresponding author: Lina E. Polvi (lina.polvi@umu.se)

Key Points:

- Boulder-bed semi-alluvial channels behave like low submergence regime mountain streams with sediment deposition upstream of boulders
- Fennoscandian semi-alluvial rapids are not re-worked (boulders transported or bedform formation) by high fluvial flows (i.e., Q_{50})
- Large grains ($>D_{84}$) are important in shaping channel morphodynamics and have implications for restoration of salmonid spawning gravel

Abstract

In northern Fennoscandia, semi-alluvial boulder-bed channels with coarse glacial legacy sediment are abundant, and due to widespread anthropogenic manipulation during timber-floating, unimpacted reference reaches are rare. The landscape context of these semi-alluvial rapids— with numerous mainstem lakes that buffer high flows and sediment connectivity in addition to a regional low sediment yield— contribute to low amounts of fine sediment and incompetent flows to transport boulders. To determine the morphodynamics of semi-alluvial rapids and potential self-organization of sediment with multiple high flows, a flume experiment was designed and carried out to mimic conditions in semi-alluvial rapids in northern Fennoscandia. Two slope setups (2% and 5%) were used to model a range of flows (Q_1 (summer high flow), Q_2, Q_{10} & Q_{50}) in a 8 x 1.1 m flume with a sediment distribution analogous to field conditions; bed topography was measured using structure-from-motion photogrammetry after each flow to obtain DEMs. No classic steep coarse-bed channel bedforms (e.g., step-pools) developed. However, similarly to boulder-bed channels with low relative submergence, at Q_{10} and Q_{50} flows, sediment deposited upstream of boulders and scoured downstream. Because the Q_{50} flow was not able to re-work the channel by disrupting grain-interlocking from preceding lower flows, transporting boulders, or forming channel-spanning boulders, the channel-forming discharge is larger than the Q_{50}. These results have implications for restoration of gravel spawning beds in northern Fennoscandia and highlight the importance of large grains in understanding channel morphodynamics.

Plain language summary

Many streams in northern Scandinavia and Finland contain abundant boulders that were originally deposited by glaciers (>10,000 year ago). However, most of these so-called ‘semi-alluvial’ streams were heavily altered during the timber-floating era. In order to understand how these streams should look naturally and change over time, experiments were conducted mimicking this stream type. An experimental stream was built in a flume (8 x 1.1 m) with down-scaled sediment sizes matching that of streams in northern Sweden. With two different slopes (2% and 5%), four flows were run to mimic flows ranging from the annual high flow to the 50-year flood. Because lakes are common along these streams, high recurrence-interval flows (that occur rarely) are not as large as in mountain streams. Therefore, boulders barely moved even with the 50-year flood at the 2% slope and only rolled slightly at the 5% slope (due to downstream scour). During 10-year and 50-year floods, finer sediment deposited upstream and eroded downstream of boulders. Contrary to mountain streams with coarse boulders, a flow much greater than the 50-year flood is necessary to re-work the channel bed. These results have implications for stream restoration, including providing habitat and spawning gravel for trout and salmon.

1 Introduction

1.1 Semi-alluvial channels

Semi-alluvial channels have commonly been described as those where a cohesive boundary, most commonly bedrock or cohesive clays, either composes the channel banks, thus confining the channel from lateral migration, or the channel bed, thus constraining the channel from degrading (Coulombe-Pontbriand & LaPointe, 2004; Meshkova et al., 2012; Turowski, 2012). Another type of semi-alluvial channel exists where the channel contains abundant cohesive or coarse sediment, which are fixed immobile points in the channel and have not been deposited by alluvial processes (Pike et al., 2018). This potentially immobile sediment has been referred to either as lag or legacy deposits in cases where mass wasting has caused an input of coarser material (e.g., Brummer & Montgomery, 2003), where lahar deposits below the channel inhibits incision (Reid et al., 2013), or where a previous geomorphic process regime, such as glaciation, has deposited sediment that is currently immobile within the current fluvial hydrological regime (Gran et al., 2013; Polvi et al., 2014). Semi-alluvial channels with glacially-derived sediment from depositional landscapes formed by continental ice sheets may contain non-alluvial patches that are (1) easily eroded and form alluvial deposits, (2) cohesive fine-grained material that only responds to extreme high flows (Pike et al. 2018), or (3) coarse-grained cobbles and boulders (Ashmore & Church, 2001; Polvi et al., 2014). Such semi-alluvial channels with till beds, containing either cohesive sediment or sand, gravel and large boulder clasts, are common on Canada’s Southern Shield and Southern Boreal Shield (Ashmore & Church, 2001) and in northern Fennoscandia (Polvi et al., 2014). In such systems, where all sediment was not deposited by fluvial processes and is potentially unable to be reworked even by high recurrence-interval high flows, it is unknown whether the mobile sediment self-organizes into predictable bedforms or whether predictable patterns of sediment clusters and scour form.

In northern Fennoscandia, boulder-bed semi-alluvial channels are common (Polvi et al. 2014; Rosenfeld et al., 2011), as the landscape has been shaped by several episodes of continental glaciation. Glacially drifted till is the most common deposit in Fennoscandia, forming various landforms in the form of ribbed and Rogen moraines, drumlins, eskers, and erratics (Seppälä, 2005). Semi-alluvial channels are found in tributary catchments to large rivers that flow from the mountains to the Baltic Sea in areas with mapped fluvio-glacial sediment in longitudinal swaths (Geological Survey of Sweden surficial geology maps, 1:25,000- 1:100,000). The tributaries are divided into three main process domains, which are spatially separate zones with distinct suites of geomorphic process (*sensu* Montgomery, 1999): lakes, slow-flowing reaches in peat or fine sediment (S_0: <0.01 m/m), and semi-alluvial rapids (S_0: 0.005-0.07 m/m) (Figure 1). Similar systems with abundant mainstem lakes and 'steeps' and 'flats' have been described by Snyder et al. (2008, 2012) in a similarly glaciated landscape in Maine, USA. Putting semi-alluvial rapids within the context of their stream network organization of process domains is necessary to understand reach-scale sediment processes. Mainstem lakes buffer sediment and water fluxes, which reduce the available fine sediment input from upstream reaches (Snyder et al., 2012) and may preclude very high flows (Leach & Laudon, 2019). Thus, to summarize, a process-based understanding of morphodynamics in semi-alluvial rapids in northern Fennoscandia is hampered by two geomorphic factors: (1) streams are semi-alluvial, in that they contain coarse glacial lag sediment (till from moraines and subglacial tunnels) and (2) numerous mainstem lakes buffer sediment and water fluxes.

Furthermore, natural reference sites are lacking due to extensive timber-floating (mid 1800s to ~1980) that caused widespread channelization and clearing of rapids, so stream restoration schemes cannot rely on copying existing reference sites. In these rapids, some of which were unimpacted and others of which were channelized and later restored, no clear pool-riffle or step-pool bedforms have been observed in the field (*personal observation*), and cascade bedforms have been observed at slopes where plane bed, alternate bar, or step-pools should form in alluvial channels (S_0: ~0.04-0.07 m/m, *sensu* Montgomery & Buffington, 1997; Palucis & Lamb, 2017). Due to the widespread nature of timber-floating, which necessitated channelization and clearing of coarse boulders (through manual clearing, the use of dynamite and bulldozers), virtually no unimpacted reference reaches exist (Nilsson et al., 2005). Most of those that were unimpacted by channelization—though were still impacted by clearing of instream wood, harvesting of old-growth riparian trees, and flow diversion—are steeper than those that have been restored (Polvi et al., 2014). In the past decade, several stream restoration projects have attempted to restore these semi-alluvial rapids because of the low salmonid populations and negative effects on biodiversity (Gardeström et al., 2013); however, very little research or knowledge on the processes governing sediment transport and organization in these streams are available (except Rosenfeld et al., 2011).

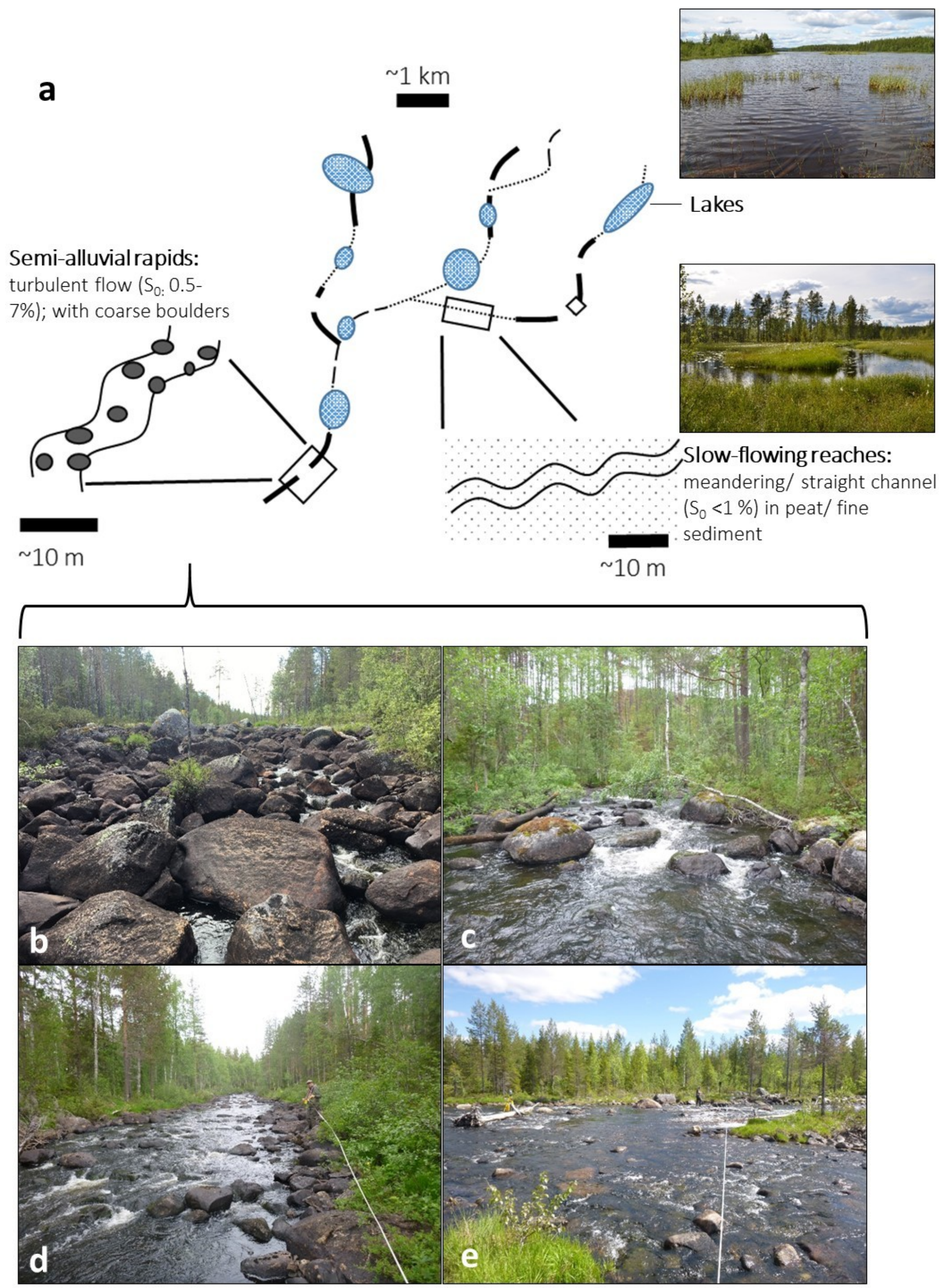

Figure 1. (a) Schematic of stream networks in tributary streams in northern Fennoscandia. Streams are segmented into three process domains: semi-alluvial rapids, slow-flowing reaches and lakes, with four examples of prototype reaches of semi-alluvial rapids (b-e). Photos b & c are of unimpacted reaches with channel bed slopes of 0.05 and 0.04 m/m, respectively; photos d & e are of restored reaches with channel bed slopes of 0.03 and 0.02 m/m, respectively. In photos b-d, the flow direction is out of the picture, and in photo e, the flow direction is from right to left.

1.2 Background

The channel geometry and bedforms found in semi-alluvial channels are not easily predicted based on slope or bankfull discharge. Forms and processes of alluvial streams, on the other hand, have been well-studied, allowing prediction of sediment transport, channel geometry, and bedforms (Church, 2006; Faustini et al., 2009). For example, regionally-derived downstream hydraulic geometry equations can be used to predict channel width, depth, and velocity based on relationships with bankfull discharge or drainage area, because these channel geometry parameters reflect the stream's equilibrium conditions (Church, 2006; Leopold & Maddock, 1953). Even in steep, coarse-bed channels, channel bed slope can predict bedform morphology (e.g., step-pools, plane bed or pool-riffle), which may reflect a balance between sediment supply and transport capacity (Montgomery & Buffington, 1997) or other processes co-varying with slope (Palucis & Lamb 2017). In addition, the formation of and the controlling mechanisms of sediment sorting in step-pools and pool-riffles have been examined, showing that these bedforms reflect a self-organization phenomenon that form in order to dissipate energy (Chin & Wohl, 2005), and that sediment is preferentially stored in and mobilized from pools (e.g, Sear, 1996).

Some insight into semi-alluvial channels with coarse glacial sediment are available from experiments based on mountain streams with boulder-bed channels. In general, the effects of boulders on local sediment transport are poorly understood due to local feedbacks between hydraulics and bed response (Monsalve & Yager, 2017; Nitsche et al., 2012; Yager et al., 2007). Finer sediment patches commonly form on the lee side of protruding clasts due to flow separation (Thompson, 2008), which in turn alter local roughness, affecting hydraulics and thus sediment transport around boulders (Laronne et al., 2001). However, in boulder-bed channels with low relative submergence ($h/D < 3.5$, where h is the flow depth and D is the boulder diameter; Papanicolaou & Kramer 2005), experimental studies have documented deposition of fine to medium-sized sediment directly upstream of boulders (Monsalve & Yager, 2017; Papanicolaou et al., 2018). Monsalve and Yager (2017) explained the formation of upstream patches as a consequence of negative shear stress divergence upstream of boulders and an increase in dimensionless shear stress downstream of boulders in channels with low relative submergence (RS); however, this study used a simplified system with regularly spaced equi-sized hemispheres, spaced so that wakes between consecutive boulders did not interfere with one another. Furthermore, the presence of protruding boulders can absorb a significant amount of shear stress so that the available shear stress for entrainment and transport of mobile sediment decreases, leading to potential overestimation of sediment transport (Papanicolaou et al., 2012; Yager et al., 2007, 2012).

On a larger spatial and longer temporal scale than sediment deposition dynamics, processes that drive bedform development and steer which flow is channel-forming may differ for semi-alluvial and alluvial channels. In steep, coarse- (gravel, cobble, and boulder) bed alluvial channels, bed slope can predict either a unique bedform or multiple stable states (Palucis & Lamb, 2017). For example, according to Montgomery & Buffington (1997), step-pool channels commonly have slopes ranging from 0.03 to 0.065 m/m; however, further studies have shown that only individual steps form at slopes around 0.04 m/m and continuous steps require slopes exceeding 0.07 m/m (Church & Zimmerman, 2007). At lower slopes, stone lines or transverse ribs form out of cobbles and boulders, without channel-spanning pools; however, these are commonly submerged even at moderate flows (Church & Zimmerman, 2007). In terms of the role of sediment, the formation of step-pools is a combination of the random location of keystones, at which other large grains come to rest (Curran & Wilcock, 2005; Lee & Ferguson 2002; Zimmerman & Church, 2001), and hydraulics, where step-pools form under antidune crests at high discharges so that scour occurs on the falling limb creating a pool between coarser deposits (Grant, 1997; Lenzi, 2001; Whittaker & Jaeggi, 1982). Based on these step-forming hypotheses, the limiting factor for forming steps in boulder-bed semi-alluvial channels will not be keystone clasts but rather the ability for additional large grains to deposit upstream of keystones and for sufficient scour to take place downstream of keystones.

Furthermore, regardless of whether step-pools or any other bedform or regular sediment cluster can form, there is the question of which flow creates and then maintains the current channel configuration, in terms of bedforms and boulder configuration. It is debated whether the effective discharge, defined as the flow that transports the most sediment over time, is also the discharge that determines the channel morphology (Andrews, 1980; Emmett & Wolman, 2001; Lenzi et al., 2006a; Torizzo & Pitlick, 2004). Although effective discharge originally referred to transport of suspended sediment (Wolman & Miller, 1960), this concept has also been applied to bedload transport (e.g., Lenzi et al., 2006a; Torizzo & Pitlick, 2004). In many alluvial channels, the bankfull flow, with a 1.5-2 year recurrence interval, does the most geomorphic work and is the flow to which the channel has adjusted (Andrews, 1980; Phillips and Jerolmack, 2016). However, depending on the system, the effective discharge for bedload may be discordant with the channel-forming flow (e.g., Downs et al., 2016) and may instead be a channel-maintaining discharge, while a more infrequent flow shapes the channel (Lenzi et al., 2006a). For example, in alluvial, snowmelt-dominated Rocky Mountain streams, the effective discharge reflects rare events (e.g., Q_{50}) in plane-bed channels, whereas the effective discharge is nearer the Q_{bf} flow in step-pool channels (Bunte et al., 2014); however, the channel-forming discharge for step-pool channels often reflects a higher recurrence-interval flow (Lenzi et al., 2006b). Similarly, in a study in formerly glaciated mountain streams of British Columbia, the effective discharge was overall very frequent but was also highly variable, depending on the threshold for gravel-sized sediment transport (Hassan et al., 2014). Hassan et al. (2014) distinguished three stream types in British Columbia based on whether there was mobile or immobile gravel or whether sand was transported over gravel. Channels with mobile gravel exceeded the effective discharge multiple days per year, channels with immobile gravel had very low-frequency, high-magnitude effective discharges, and those with mobile sand but immobile gravel showed a bimodal effective discharge. Therefore, there may be a low effective discharge that does not, however, equal the channel-forming discharge. In addition, the presence of large boulders and thus low relative submergence increases the flow resistance (Bathurst, 2002). For example, the most accurate equations to predict the grain component of flow resistance require the D_{84} in addition to D_{50} (Bray, 1979; David et al., 2011; Hey, 1979). Thus the available shear stress to mobilize sediment is reduced (Yager et al. 2007). Therefore the potential of flows to transport sediment decreases which should increase the channel-maintaining or channel-forming discharge.

Predictions of potential sediment transport and channel re-working depend not only on shear stresses associated with different flow magnitudes, but also on the flow history since a channel-reworking flow (Masteller et al., 2019). During low-magnitude flows, sediment is locally rearranged and particle interlocking increases, thus increasing the critical shear stress for particle movement (Reid et al., 1985). However, during high-magnitude flow events, particle interlocking is disrupted and the critical shear stress decreases, allowing for much higher transport rates (Turowski et al., 2009; Masteller et al., 2019). Thus, the probability of sediment transport depends on prior flows, including the time since a high-magnitude, sediment transporting flow (Masteller et al., 2019; Yager et al., 2012), which may thus account for a large portion of the variability in dimensionless shear stress values (Johnson, 2016). Therefore, when determining whether a flow is capable of re-working the channel, the probability of a high flow reworking the channel decreases if a channel has experienced previous low or medium flows. So, a more conservative estimate (avoiding underestimations) of a channel-forming flow should be based on a channel where the sediment has been locally rearranged with particle interlocking thus exhibiting a critical shear stress on the higher end within the range of variability.

1.3 Objectives

In order to gain insight of the morphodynamics of semi-alluvial boulder-bed channels , a flume study was designed and carried out to mimic conditions in previously field-studied semi-alluvial rapids in northern Sweden (Polvi et al., 2014). The objective of this study was to model the potential evolution of bedforms or self-organization of sediment in semi-alluvial channels with coarse glacial legacy sediment using a range of flows (annual high-flow to 50-year flood) in a flume at two different slopes (0.02 and 0.05 m/m). I aimed to answer the following questions: (1) given a history of potentially stabilizing, low flows, can we determine the potential range of channel-forming discharges? Specifically, is a large-magnitude flow (e.g., Q_{50}) capable of reworking the channel, transporting boulders and creating bedforms? Here, I define channel-forming discharge as a flow that can transport boulders and re-organize potential bedforms or sediment clusters. This question is addressed through observations of potential boulder transport and by calculating the event-based and cumulative geomorphic work by each flow given a specific order of flows. Whether or not the geomorphic work during the Q_{50} flow exceeds that of the Q_1 or Q_2 flows will determine whether the higher flow is capable of re-organizing the bed. (2) Do patterns of sediment erosion and deposition form around large, potentially immobile boulders? This builds on the literature of boulder-bed channels in low relative submergence regime systems. These results will provide management recommendations on how to best restore these semi-alluvial channels in a self-sustaining manner.

1.4 Prototype description

The flume study modeled semi-alluvial boulder-bed stream channels found in tributaries to the free-flowing Vindel River, which with a drainage area of ~12,500 km^2 is the largest tributary to the Ume River that flows into the Baltic Sea from the Scandes Mountains at the Swedish-Norwegian border. From the mid-1800s to the 1970s, the stream networks were used as a transport system for timber from the inland forests to the coastal sawmills, and thus nearly all semi-alluvial channels were channelized. Channelization involved manual clearing of coarse sediment, closing off side channels, building levees with coarse sediment (cobbles and boulders), and later using bulldozers to clear the middle of the channel. Restoration started in the 1990s with ‘basic restoration’ that entailed returning coarse sediment from levees to the main channel and opening up some side channels (Gardeström et al., 2013). In 2010, ‘enhanced restoration’ commenced that involved significantly widening the channel and obtaining large boulders (>1 m) from the surrounding forest that were placed into the channel in addition to the cobbles and boulders that remained along the channel edge (Gardeström et al., 2013). Although virtually all semi-alluvial rapids were channelized, some unimpacted reaches remain but most of them are steeper than those that were channelized and subsequently restored (Polvi et al., 2014).

In this study, two prototype channels were used, representing enhanced restored reaches (note: enhanced restored reaches are referred to as 'demo restored' reaches in Polvi et al., 2014) and unimpacted reaches (Figure 1). Channel geometry and sediment distribution parameters were obtained from four unimpacted and five enhanced restored stream reaches described in more detail in Polvi et al. (2014). The average channel bed slope of the enhanced restored reaches was ~0.02 m/m (range: 0.015-0.037 m/m), whereas unimpacted reaches had an average slope of ~0.05 m/m (range: 0.029-0.074 m/m). The remainder of the channel geometry parameters, including width, depth and sediment distribution, was similar between the two groups of reaches (Polvi et al., 2014); channel widths range from 7-20 m and average bankfull depths are 0.5-1 m. The catchments, which vary in drainage area from 9-151 km^2, consist of an average of 2.53% lakes (0.04-6.65%), all of which are connected to the stream network, and an average of 21% wetlands (6.00-52.40%) (SMHI, 2015). Sediment distributions were obtained from 300-particle pebble counts of the nine reaches. The average median grain size was 245 mm (range: 130-400 mm), average 84th percentile sediment size was 624 mm, and average maximum sediment size was 1670 mm (range: 1400-5000 mm). There was less than 10% sand, and examination of the sub-surface sediment did not reveal higher percentages of sand; i.e., there is not substantial armoring that shields a buried sand layer. This is further supported by the low rates of weathering and sediment production in the region, as suggested by global-scale sediment yield maps (Lvovich et al., 1991; Walling & Webb, 1983) and quantification of annual sediment flux in a nearby catchment of only ~55 t/km^2 (Polvi et al., 2020), which is due to the relatively low relief, crystalline bedrock (and till), and cold climate. Because of the segmented channel network, where mainstem lakes are abundant, there is probably very little sediment transport of fine grain sizes from upstream high-gradient reaches (Arp et al., 2007).

The flow regime in northern Sweden is dominated by snowmelt-runoff high flows in the spring/early summer. The average annual precipitation is 600 mm, of which 40% falls as snow (SMHI, 2017). The numerous mainstem lakes serve to buffer high flows, therefore low-recurrence interval floods do not substantially increase in magnitude compared to higher-recurrence interval floods, as seen in ratios of recurrence interval flows (Bergstrand et al., 2014). For example, the Q_{50} flow is less than twice that of the Q_2 flow ($Q_{50}/Q_2 = 1.8$), and even the predicted Q_{100} and Q_{500} flows are only 1.12 and 1.4 times that of the Q_{50} flow, respectively (Figure S1). Ice forms in most of these channels during winter, as either surface or anchor ice and flooding due to ice cover and ice jamming is also common (Lind et al., 2016). Although there are few studies studying the role of ice formation and break-up on sediment transport, Lotsari et al. (2015) found that boulders (up to 2 m in diameter) embedded in ice can be transported downstream during ice break-up. Polvi et al. (2020) quantified the amount of sediment transport under ice and during ice break-up as ~5% of annual sediment yield. However, the potential effect of ice varies within a catchment, as no anchor ice forms and little surface ice forms in reaches close to an upstream lake (Lind et al., 2016).

2 Methods

2.1 Flume setup

A mobile-bed physical model of the semi-alluvial prototype streams in northern Sweden was set up in an 8-m long, 1.1-m wide fixed-bed flume at the Colorado State University Engineering Research Center in Fort Collins, Colorado, USA (Figure 2). Using a geometric (y_r and z_r) scaling factor of 8, the initial sediment distribution was scaled-down to be analogous to that in the semi-alluvial prototype streams, and because the flume D_{10} was 4 mm and D_{min} was 0.14 mm, all sizes were sand-sized or above so there were no issues with cohesiveness (Table 1). No sediment feed was provided from upstream, creating clear water conditions, and this is consistent with the prototype field conditions with very low levels of suspended sediment or annual sediment flux (Polvi et al., 2020) and little sediment input from the hillslopes or upstream reaches. Two flume setups were used with initial bed slopes of 0.02 and 0.05 m/m, respectively. Before the flows were run, the grain size distribution was thoroughly mixed in the flume, and checks were made to ensure equal sediment depth and the desired slope throughout the flume length. For each slope, four runs were conducted with flows analogous to the summer high (Q_1), the 2-year (Q_2), 10-year (Q_{10}), and 50-year (Q_{50}) flows in the prototype streams. The flows were run in a sequence from the lowest to highest flow, with initial bed conditions for each flow equal to that of the final conditions of the preceding flow. The summer high flow (Q_1) was not based on a bankfull flow that filled the banks in the flume channel, but rather based on field conditions in the prototype channels. Flow measurements were taken in the field at the summer high flow, which was close to or just below the geomorphically-defined bankfull flow (Gardeström J., *unpublished data*) (see Section 2.2. for a full description of flows). Each flow was run for 60 minutes, which surpassed the time necessary until equilibrium conditions were met, as defined by minimal to no visible sediment transport or transport out of the reach. As no boulder (>D_{84}) movement was detected (other than slight rotation, as described in Results) during any flow, equilibrium conditions were only based on transport of the fine sediment fraction. After each flow, the bed topography and channel geometry were measured (described below in Section 2.3) before running the next higher flow. After the flume's slope was altered from 0.02 to 0.05 m/m, sediment lost from the previous slope setup was returned and all sediment was manually mixed with shovels, so that the initial conditions for both slopes were approximately the same, with a plane bed and well-mixed sediment sizes. This experimental setup means that initial conditions were different for the two slopes and for each flow. However, due to the wide sediment size distribution, it would be nearly impossible to replicate initial conditions for each flow and slope. Therefore, the results should not be used to compare processes between slopes but to be used as two case studies of boulder-bed semi-alluvial reaches. The bed degraded slightly during each subsequent flow, as seen through an increase in slope: for the 2% slope setup, the centerline slope started at 0.022 m/m and changed to 0.0211, 0.0223, 0.0226, and 0.0222 m/m with each consecutively higher flow; for the 5% slope setup, the centerline slope started at 0.0532 m/m and changed to 0.0538, 0.0538, 0.0549, and 0.0545 with each consecutively higher flow. However, this reach-scale degradation is fairly minor in terms of changing initial conditions for each flow, and the centerline slope was controlled more by local sediment re-arrangement rather than reach-scale degradation. With this setup, channel width could not adjust; however, due to the coarse sediment sizes, it is assumed that adjustment of the channel would occur via downstream sediment transport rather than streambank erosion and lateral migration.

Figure 2. Photos of each flume run at two slope setups with four different flow magnitudes. Pictures a-d were taken at the 2% slope setup, and pictures e-h were taken at the 5% slope setup. Photos a & e were taken at Q_1 (0.006 m^3/s); photos b & f at Q_2 (0.017 m^3/s); photos c & g at Q_{10} (0.025 m^3/s); and photos d & h at Q_{50} (0.031 m^3/s).

Table 1. Prototype Reach Characteristics and Corresponding Flume Specifications

	Prototype reach characteristics	**Flume specifications**
Bed Slope	Restored channels: 0.8-3.7% Unimpacted channels: 2.9-7.4%	Setup 1: 2% Setup 2: 5%
Width	8.8 m	1.1 m
Length	64.0 m	8.0 m
Sediment Input	Crystalline rocks, low levels of weathering, and abundant lakes that buffer sediment = low levels of suspended sediment	Clear water (no sediment feed)
Initial Conditions	Rapids form in poorly sorted till within moraines and eskers	Unsorted sediment mix, with plane bed morphology
	Sediment size distribution	
D_{16}	56 mm	7 mm
D_{50}	248 mm	31 mm
D_{84}	624 mm	78 mm
D_{max}	1672 mm	209 mm
	Flows/unit discharges	
Q_1	1.0 m^3/s / 0. 125 m^2/s	0.006 m^3/s / 0.005 m^2/s
Q_2	3.1 m^3/s / 0. 062 m^2/s	0.017 m^3/s / 0.015 m^2/s
Q_{10}	4.6 m^3/s / 0.577 m^2/s	0.025 m^3/s / 0.023 m^2/s
Q_{50}	5.6 m^3/s / 0.705 m^2/s	0.031 m^3/s/ 0.028 m^2/s

2.2 Flume flows

For each of the four unimpacted and five enhanced restored stream reaches studied in Polvi et al. (2014), the various flow magnitudes that represent the Q_2, Q_{10} and Q_{50} flows were derived from a hydrological model, S-HYPE, developed by the Swedish Meteorological and Hydrological Institute (Lindström et al., 2010; SMHI, 2015). The model (HYdrological Predictions for the Environment) makes sub-basin scale hydrological calculations based on the basin-characteristics of surficial geology, landuse, altitude, lake depth, and stream length, and temporal inputs of sub-basin mean daily temperature and precipitation (Lindström et al., 2010). The average of each of these flows for the nine reaches were used to calculate the desired discharge for the flume runs. The Q_1 flow magnitude was based on high flow field-measurements of enhanced restored streams (Gardeström J., *personal communication*); although this may not equate to a flume channel-filling flow, it is analogous to the flow magnitude experienced by the prototype channel most years directly after the snowmelt-induced spring flood. The experimental flows were scaled down by a factor of 181.02 according to equation (1) following Froude number similitude over fixed beds (Julien, 2002).

$$Q_r = y_r z_r^{\frac{3}{2}} \qquad (1)$$

where, Q_r is the discharge scaling factor, and y_r and z_r are the lateral and vertical scaling factors, respectively, which were both set to 8.

Although the objective of this study was to model temporal evolution of the bed and potential bedforms, scale effects used for mobile bed Froude models was not deemed to play a significant role. Because the main objective of scaling the discharge was to obtain relative changes in flow that correspond to different recurrence intervals in the field, exact correspondence to a specific flow was not necessary. Also in Froude scaling, non-dimensional shear stress scales directly, thus entrainment of model particles will be equal to that in the field. For each flume setup, a low-flow discharge was run first to provide saturated conditions prior to the experimental runs. Discharge was measured in a closed pipe prior to the inflow in the flume using a Badger-meter M2000 flow meter. Before entering the flume, the inflow was allowed to mix in a 'crash box' for ~0.5 m to dampen turbulence before entering the flume. The top 0.5 m of the flume was lined with very coarse sediment so that preferential scour and sediment entrainment did not occur where the water first entered the flume over a lip. Morphologic measurements started downstream of the coarse sediment buffer zone. Likewise, at the downstream end of the flume, sediment was preferentially transported as a headcut formed. However, the morphologic analyses were cut off where this effect was seen.

2.3 Morphologic & hydraulic data acquisition and analyses

Structure-from-motion photogrammetry (SfM) was used to create digital elevation models (DEMs) of bed topography (Westoby et al., 2012). SfM-created DEMs were constructed before all runs at each slope setup and after each run, with progressively higher flows. For each flume setup with different slopes, a terrestrial LiDAR scan (TLS) was used to determine a coordinate system and be able to georeference the SfM scans, based on targets affixed to the flume walls. The TLS scans provided exact xyz coordinates of the targets, which were used to georeference the SfM-based DEMs. A Canon EOS Rebel T3i DSLR camera with a fixed, non-zoom lens (Canon EF-S 24 mm prime lens), which minimizes edge distortion of photos, was mounted to a movable cart on rails ~30 cm above the flume bed. Photos were taken ~20 cm apart looking upstream and downstream at an oblique 45° angle. This flume setup and sediment distribution was included in a study comparing results from SfM and TLS scans, which found that SfM can produce topographic point clouds with comparable quality and greater point densities to TLS (Morgan et al., 2017), thus verifying the validity of the SfM scans in this study. The images were processed using AgiSoft PhotoScan Professional (Agisoft LLC, 2014) to obtain topographical point clouds.

The topographical point clouds were imported into ArcMap 10.5.1 (ESRI, 2017) and rasters were created with a grid size of 5 mm to create digital elevation models (DEMs) of the topography for the initial conditions at each slope setup and after each flow with a precision of 2 mm (Polvi, 2020; Figure 3). In areas with missing data, the neighboring points were iteratively averaged to interpolate elevations for pixels. The flume study area was clipped to 7.0 m and 6.3 m in length for the 2% and 5% slope setups, respectively, to remove the upstream turbulent section containing much coarser sediment and a headcutting section at the downstream portion of the flume. To analyze differences in aggradation versus degradation after each run, the DEMs were subtracted from one another to create DEMs of difference (DoDs) (Wheaton et al., 2010); DoDs were created comparing each flow to the initial conditions and after each successive flow.

In addition, all large clasts, defined as sediment clasts >D_{84} (~80 mm in diameter), were digitized (Polvi 2020), and the spatial distribution of aggradation and degradation in relation to the large clasts were analyzed by creating buffers equal to half the diameter of the respective clasts. Each buffer was then split into an upstream and downstream half, and the mean elevation change in each upstream and downstream buffer was calculated using zonal statistics within ArcGIS. One-sample t-tests were used to determine whether the mean elevation change in all of the upstream and downstream buffers after a given flow, compared to the previous flow and compared to the pre-flow conditions, were significantly different from 0. Two-sample t-tests were used to determine whether the mean elevation change differed between the upstream and downstream buffers for a given flow compared to the previous flow and compared to the initial conditions. Although some downstream buffers were close to or slightly overlapped with an upstream buffer for another clast, or vice versa, the effect of other large clasts in the vicinity of a buffer may contribute to variation in the mean values but should not affect the overall mean values. All statistical analyses were performed using the statistical software 'R' (RStudio Team, 2016).

The total geomorphic work done by each flow was calculated as the sum of the volume of aggradation and degradation in the entire flume area, which is different than the standard method of using transport rates and assumes that large channel changes implies relatively high transport rates. Because the flows were run in order from lowest to highest for each slope setup, the geomorphic work for the higher flows may be underestimated due to interlocking of grains during lower flows (e.g., Masteller et al., 2019); therefore, the geomorphic work for each flow is also reported as the cumulative combined aggradation and degradation of that flow in addition to all prior flows. To determine how much the sediment was reworked after each flow, the percent of the flume area that experienced erosion or deposition was calculated by determining how many pixels (5 mm x 5 mm) in DoDs experienced >0.01 m or < -0.01 m of elevation change and by transforming this to a percent of the entire bed. Thresholding of the DoDs was only done for visualization purposes (Figures 4a, S2, S3) and for calculation of the area affected by erosion or deposition (>0.01 m of elevation change). For the volume analysis of erosion/deposition, potential errors would contribute to negligible or small volumes compared to actual change. For the D_{84} buffer analysis, random errors should cancel each other out (positive and negative change) in calculation of mean elevation change. DEMs were detrended to visualize topography throughout the entire reach (Figure 3). Using the detrended DEMs, topographical roughness was calculated as the standard deviation of elevation values.

Because the main objective of this flume experiment was to analyze changes in morphology, detailed hydraulic measurements were not made. However, flow depths were recorded longitudinally spaced throughout the channel and at three lateral locations during each flow. Missing flow depth data from the first two flows at the 2% slope setup were estimated using time-lapse photos during the runs and DEMs by measuring flow depths based on the water surface elevation. Reach-scale averages of flow depth were used to calculate the reach-averaged shear stress (Equation 2), relative submergence, and Froude number. Because the critical shear stress required to entrain larger than D_{50} grain sizes does not increase linearly, but is lower due to protrusion effects (e.g., Ashworth & Ferguson, 1989), only the dimensionless shear stresses (τ^*) on D_{50}-sized sediment for each flow and slope were calculated using Shield's equation (Equation 3). These values were then compared with critical dimensionless shear stress (τ_c^*) values of 0.1, which may be more accurate for steep streams with low relative submergence

(Lenzi et al., 2006b), and those calculated based on Lamb et al.'s (2008) slope-dependent regression (Equation 4).

$$\tau = \rho_w g h S \tag{2}$$

where, τ is the reach-scale shear stress (N/m^2), ρ_w is the density of water (1000 kg/m^3), g is acceleration due to gravity (9.81 m/s^2), h is the average flow depth, and S is the reach-averaged bed slope.

$$\tau * ¿ \frac{\tau}{(\rho_s - \rho_w) g D_{50}} \tag{3}$$

where, τ* is the dimensionless shear stress, D_{50} is the median grain size (m), τ is the reach-scale shear stress (N/m^2), ρ_s is the density of sediment (2650 kg/m^3), ρ_w is the density of water (1000 kg/m^3), and g is acceleration due to gravity (9.81 m/s^2).

$$\tau * ¿_c = 0.15 S^{0.25} ¿ \tag{4}$$

where, $\tau*_c$ is the critical dimensionless shear stress and S is the bed slope (m/m) (Lamb et al., 2008).

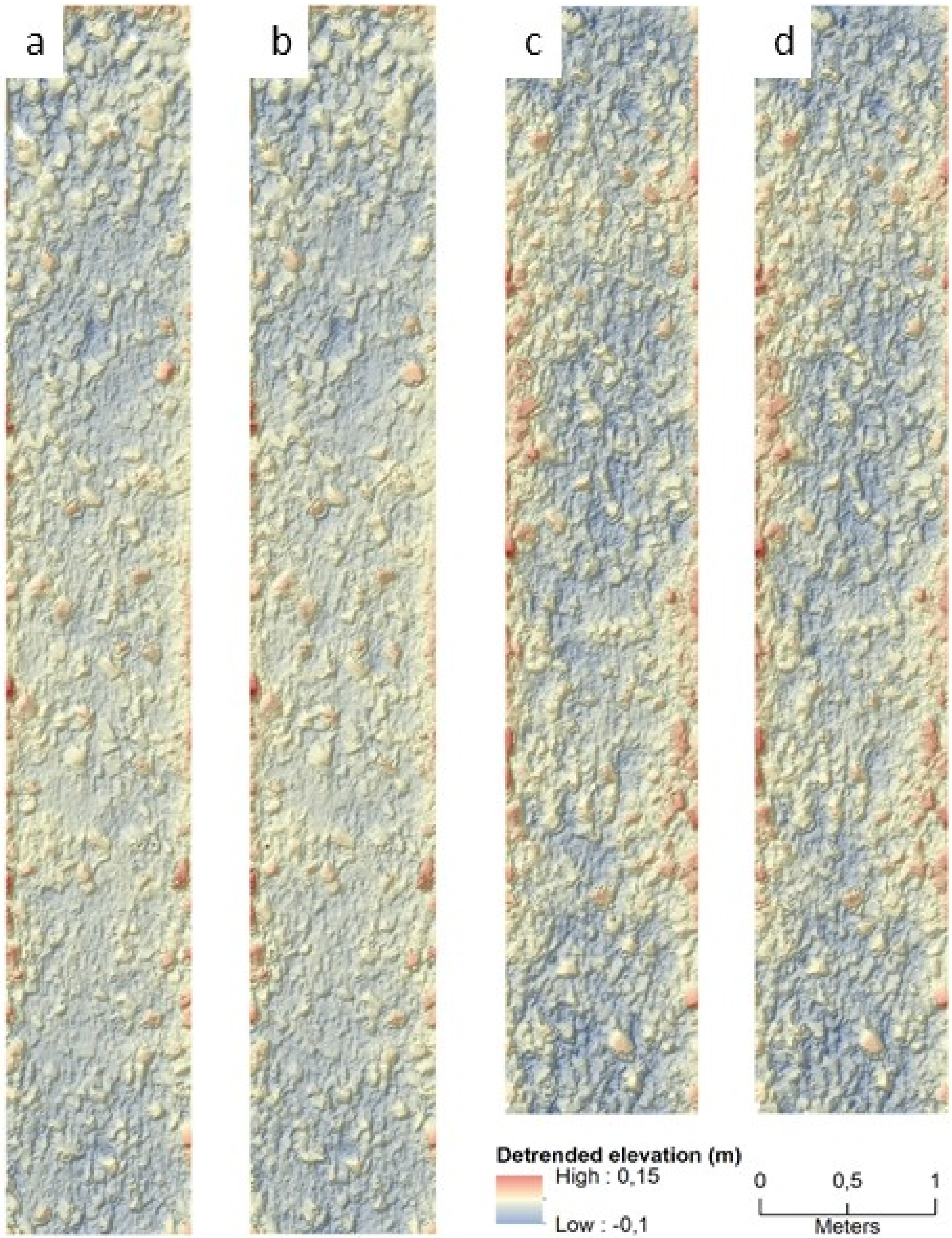

Figure 3. Detrended digital elevation models based on structure-from-motion photogrammetry at the 2% slope setup (a & b) and 5% slope setup (c & d), showing initial conditions (a & c) and channel bed topography after the Q_{50} flow (b & d). Color scales show relative detrended elevations in meters. Distance scale bar applies to all DEMs. Note that the analyzed flume area was slightly shorter with the 5% slope setup due to the larger affected area by headcutting.

3 Results

3.1 General visual observations

At both slope setups, the large clasts (>D_{84}) were basically immobile, with some downstream rotation and imbrication observed at the Q_{50} flow at the 5% slope due to scour downstream of boulders. Medium-sized sediment (~D_{50}) also showed imbrication at the Q_{10} and Q_{50} flows at both slopes; imbrication was located directly upstream of large clasts or independent of the hydraulic influence of boulders (Figure 4b; 4c). Most sediment transport occurred at the beginning of each flow, and mobile sediment was quickly deposited in shielded or stable locations, inhibiting potential further transport until the next higher discharge was run. Sediment clusters of small- to medium-sized sediment (~4-20 mm), corresponding to grains sizes between the D_{10} and D_{50}, were observed upstream of immobile clasts after the Q_{10} flows at both slope setups, with corresponding scour downstream of immobile clasts (Figure 4). . Because the large clasts remained immobile at all flows, no classic bedforms, including steps, developed in these experiments; however, the formation of small-scale bedforms and structures around boulders are discussed below (section 3.3).

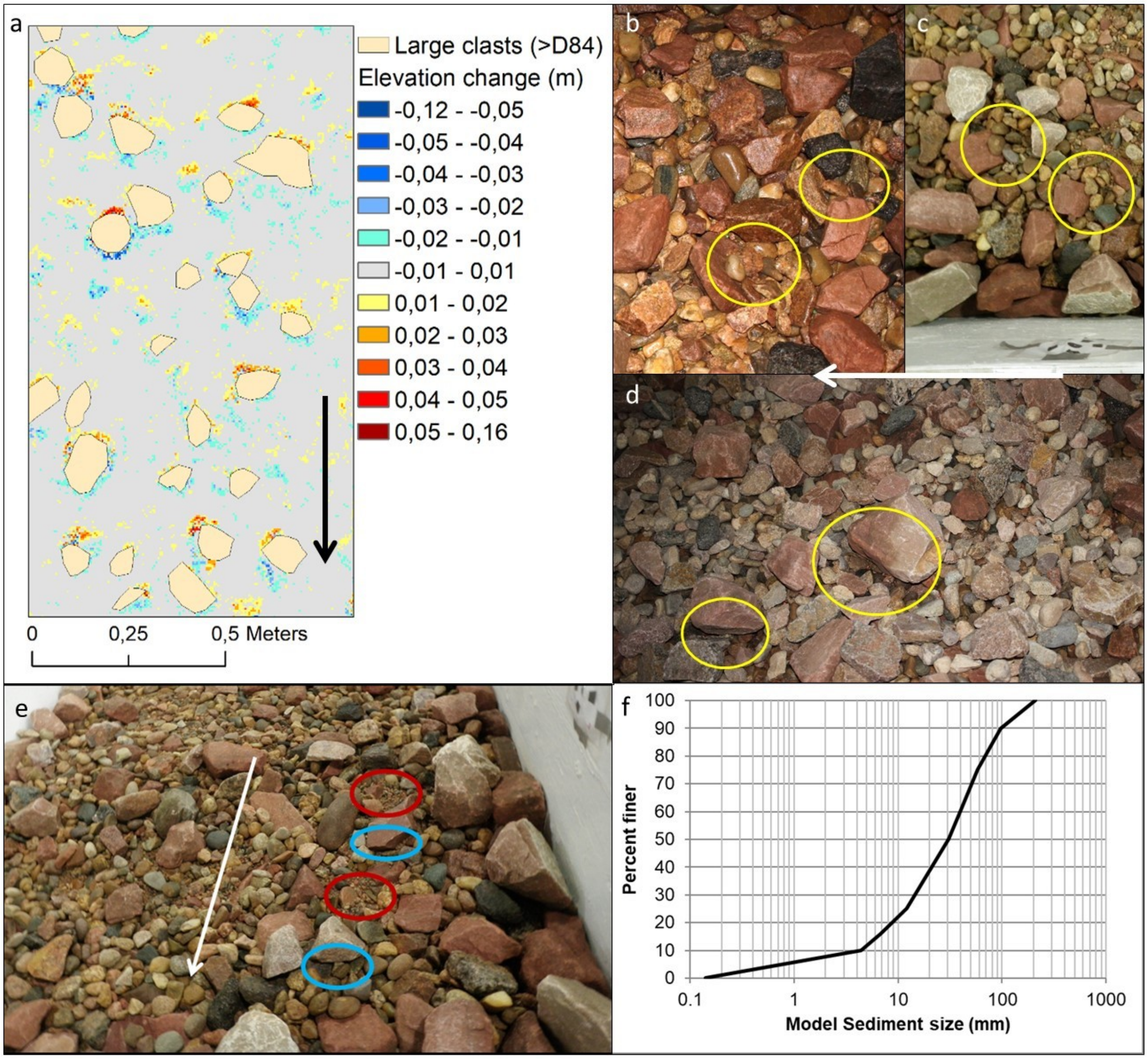

Figure 4. Patterns of erosion and sedimentation after flume runs: a) elevation change after Q_{10} flow at 2% slope setup around large clasts (>D_{84}). Photos (b & c) show imbrication, both after Q_{10} flow, at 5% and 2% slope setups, respectively. (d) Scour forms downstream of large clasts after Q_{50} flow at 5% slope setup, which caused slight downstream rotation of large clasts. (e) Photo after Q_{10} flow at 2% slope setup showing patterns of sedimentation (red) and scour (blue) around large clasts. (f) Sediment size distribution for flume experiments. See Polvi et al. (2014) for range of grain size distributions for enhanced (referred to as 'demo') and unimpacted reaches. Arrows indicate flow direction.

The relative submergences (RS) of large boulders (>D_{84}) differed for each flow but were similar between slope setups (Figure 2; Table 2); RS values were calculated for the D_{84} clast size and is therefore lower for larger clasts. At the Q_1 flow, the RS was very low (0.31 and 0.32) at both slopes; a few surface waves were evident at the 5% slope but very little turbulence or surface waves were evident at the 2% slope. At Q_2, wakes start to form downstream of boulders, and the RS was ~0.6. The RS at the Q_{10} flow was approaching 1 at the 2% slope (0.87 for D_{84}) and ranged from ~0.8-1.2 for the 5% slope with clear boulder-affected wakes forming. At the Q_{50} flow, all boulders were nearly submerged at both slopes. At the 2% slope, the RS = 1.0 and waves and wakes formed downstream of boulders; at the 5% slope, the average RS was calculated to be less than 1 but according to visual observations seemed to range from 1-1.5 with very turbulent flow. All reach-scale Froude numbers were below 1 (Table 2), but there was variation throughout the reach with local zones of critical and supercritical flow around clasts >D_{84}, particularly at Q_{10} and Q_{50} flows.

3.2 Summary of aggradation/degradation results

Less than 20% (7.13- 19.91%) of the flume area was re-worked through erosion or deposition (>0.01 m positive or negative elevation change) during each flow for both slope setups (Table 3). At the 2% slope, 3.40-9.80% of the flume area was eroded after each flow, and 1.58-7.60% of the flume area experienced deposition. At the 5% slope, 4.93-10.39% of the flume was eroded, and 5.85-11.26% of the flume area experienced deposition.

At the 2% slope, the Q_{10} flow does the most amount of work (0.044 m^3), followed closely by the Q_1 flow (0.042 m^3) (Table 3). This was visually observed during the flume runs as the bankfull flow was able to mobilize fine sediment. Because there was no input of fine sediment during or between the runs at a given slope, by the time the highest flow (Q_{50}) was run, all potentially mobilized sediment had either already been transported out of the system or settled into a shielded or non-mobile position. With little available fine sediment, combined with the Q_{50} flow not being competent enough to start mobilizing the large clasts (>D_{84}), the largest flow, Q_{50}, actually does the least amount of work (0.028 m^3). Because it would not have been possible to re-create the exact same initial conditions with such a wide grain size distribution (Figure 4f), the closest estimation of comparing the work by each flow from initial conditions is by calculating cumulative geomorphic work. Here, the cumulative Q_{50} flow (representing the sum of work by the Q_1, Q_2, Q_{10} & Q_{50} flows) eroded and deposited ~3.5 times as much sediment as the Q_1 flow but only 1.2 times that of the cumulative Q_{10} flow (sum of Q_1, Q_2 & Q_{10} flows) (Table 3; Figure S2).

At the 5% slope, the Q_{50} flow does the most amount of geomorphic work , followed in descending order by the Q_1, Q_2, and Q_{10} flows. As noted by visual observations of the flume runs and the DoDs, at the Q_{50} flow, the largest clasts start to mobilize by rolling slightly (due to downstream scour); but the other flows show the same process as with the 2% slope, where the potentially mobile sediment has already been moved. Considering cumulative geomorphic work, the Q_{50} flow eroded and deposited ~3.5 times as much sediment as the Q_1 flow and 1.6 times that of the Q_{10} flow at the 5% slope (Table 3; Figure S2).

The shear stress for the Q_1 flow at the 5% slope was roughly the same as that of the Q_{10} flow at the 2% slope. At the Q_2 flow at the 5% slope, the shear stress (22.3 N/m^2) already exceeded that of the shear stress at the Q_{50} flow at the 2% slope (13.36 N/ m^2) (Table 2); however, the geomorphic work did not differ greatly between slopes for the same flows, likely because shear stresses were not sufficient to entrain the coarser fractions even at the 5% slope (Table 2). Dimensionless shear stress values for D_{50} grain sizes at the 2% slope did not exceed 0.027, and thus were only approximately 50% of the slope-dependent τ_c* value of 0.056 (*sensu*

Lamb et al. 2008) and <30% that of 0.1 (Lenzi et al. 2006b).. The same analysis for the D_{50} at the 5% slope results in τ^* values of 0.024-0.058, which is also substantially lower than than the τ_c^*-value of 0.071 (*sensu* Lamb et al. 2008) or 0.1.

Table 2. Hydraulic & Shear Stress Parameters

Slope	Flow	Q (m^3/s)	Stream power Ω (N/s)	Froude #	Mean flow depth (m)	Relative submergence (d/D_{84})	τ (N/m^2)	τ^* for D_{50} mobilization
2%	Q_{bf}	0.006	1.18	0.47	0.024	0.31	4.48	0.009
	Q_2	0.017	3.34	0.45	0.049	0.63	8.87	0.018
	Q_{10}	0.025	4.91	0.41	0.068	0.87	11.83	0.024
	Q_{50}	0.031	6.08	0.42	0.078	1.00	13.36	0.027
5%	Q_{bf}	0.006	2.94	0.43	0.025	0.32	11.88	0.024
	Q_2	0.017	8.34	0.45	0.050	0.64	22.30	0.044
	Q_{10}	0.025	12.26	0.51	0.058	0.75	25.91	0.052
	Q_{50}	0.031	15.21	0.52	0.067	0.856	29.20	0.058

Table 3. Erosion, deposition and geomorphic work calculations

Slope	Pre-flow	Flow	Q (m^3/s)	Std. Dev. DEM (m)	Flume area with deposition (%)[a]	Flume area with erosion (%)[a]	Flume area with erosion or deposition (%)[a]	Volume of aggradation (m^3)	Volume of degradation (m^3)	Geomorphic work (m^3)[b]	Cumulative geomorphic work (m^3)[c]	Cumulative work per area (m)
2%		Pre		0.0228								
	Pre	Q_1	0.006	0.0231	4.83	9.80	14.63	0.013	-0.029	0.042	0.042	0.006
	Q_1	Q_2	0.017	0.0228	1.58	5.55	7.13	0.019	-0.017	0.036	0.079	0.011
	Q_2	Q_{10}	0.025	0.0229	7.60	7.91	15.51	0.022	-0.021	0.044	0.122	0.017
	Q_{10}	Q_{50}	0.031	0.0228	4.32	3.40	7.73	0.015	-0.013	0.028	0.150	0.021
5%		Pre		0.0304								
	Pre	Q_1	0.006	0.0308	5.85	7.07	12.92	0.017	-0.020	0.037	0.037	0.005
	Q_1	Q_2	0.017	0.0307	6.08	4.93	11.01	0.019	-0.015	0.034	0.071	0.010
	Q_2	Q_{10}	0.025	0.0306	11.26	7.48	18.74	0.006	-0.003	0.010	0.080	0.012
	Q_{10}	Q_{50}	0.031	0.0303	9.52	10.39	19.92	0.024	-0.027	0.050	0.131	0.019

[a] % area of deposition and erosion defined as area that experienced > 0.01 m net positive or negative elevation change.
[b] Geomorphic work is defined as the cumulative sum of absolute values of aggradation and degradation after each flow.
[c] Cumulative geomorphic work is defined as the sum for the given flow with all previous flows.

3.3 Erosion and deposition next to large clasts

Statistically significant differences in the mean elevation change of upstream and downstream buffers around large clasts (>D_{84}) were found at both slope setups, and similar trends were observed between each of the flows at both slopes, indicating patterns of sediment organization in relation to large immobile clasts (Figure 4, 5, S3, S4). After the Q_1 flow, significant degradation occurred in both the downstream and upstream buffers at the 2% slope, whereas there was only significant degradation in the downstream buffer at the 5% slope. Only the 5% slope showed significant differences in the upstream and downstream buffer after Q_1, with more aggradation upstream. Both slope setups showed significant differences after the Q_2 flow with more aggradation in the downstream buffers, but at the 5% slope there was no significant change in elevation in the upstream buffers. The Q_{10} flow showed significant upstream buffer aggradation at both slopes and significant degradation in the downstream buffers at the 2% slope. The opposite trend was evident at the Q_{50} flow at the 5% slope with degradation in upstream buffers; at the 2% slope, significant, yet minimal, aggradation was found in both upstream and downstream buffers.

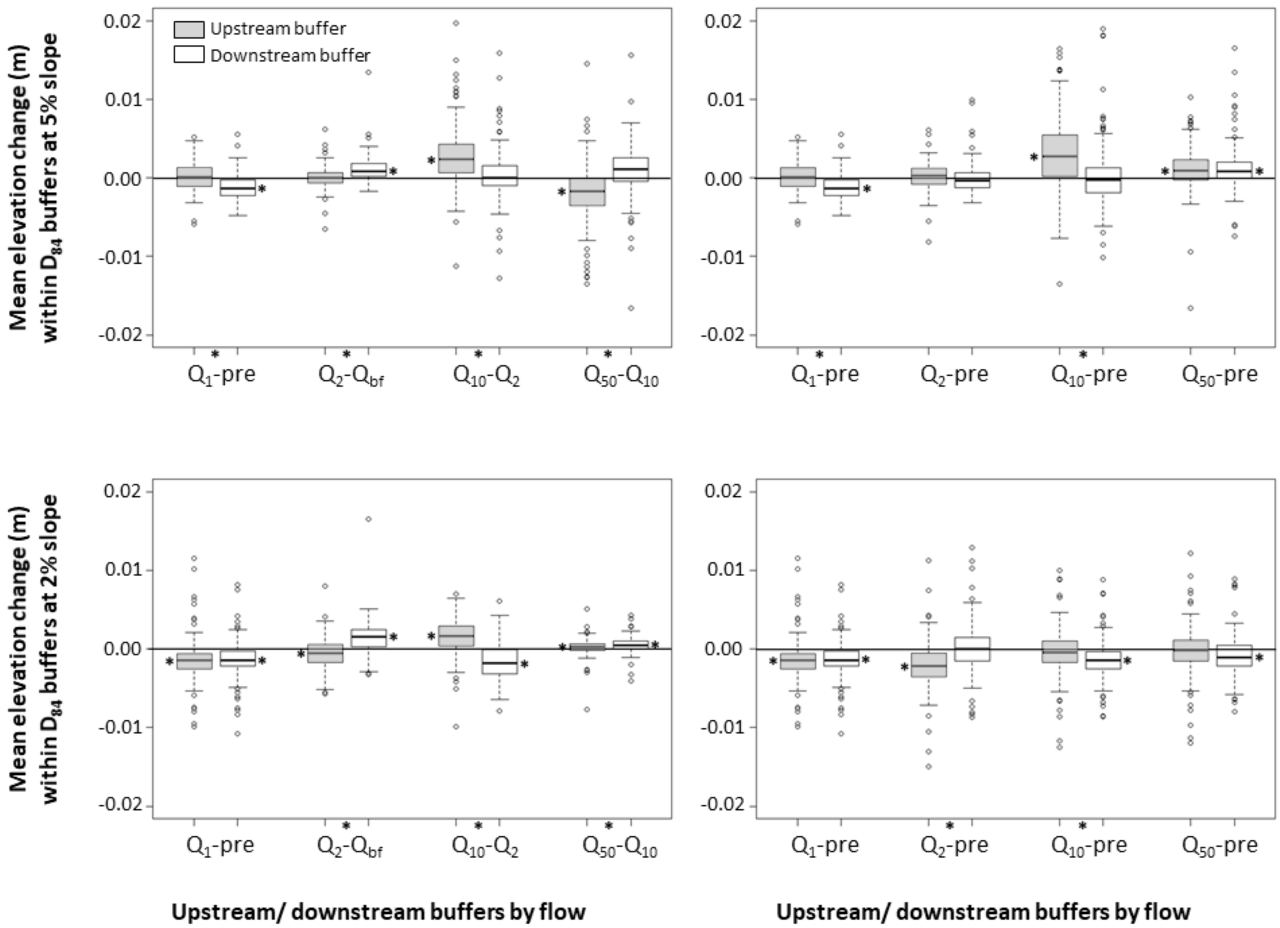

Figure 5. Boxplots of mean elevation change (i.e., aggradation/degradation) in buffers upstream (grey) or downstream (white) of D_{84} clasts. Boxplots on left show comparisons between previous flow and boxplots on right show comparisons between each flow and pre-flow conditions. Asterisks next to boxplots denote that mean is significantly different from 0 at (α=0.05) and asterisks between labels on x-axis denote that there is a significant difference between the mean elevation change in the upstream and downstream buffers.

4 Discussion

4.1 Geomorphic work and channel reworking

This flume experiment was designed to elucidate how semi-alluvial boulder-bed channels with a snowmelt-dominated flow regime evolve in terms of potential bedforms or sediment clusters. The first aspect of determining what controls channel evolution in these channels was to examine whether it is possible to determine which flow is the channel-forming discharge within the present flow regime. These flows were modeled with clear-water conditions, which was considered representative of what these channels experience in northern Sweden. This low sediment supply is due to a combination of the low sediment production in the landscape and lakes along the stream network that buffer sediment coming from upstream. Therefore, the order of the flows, which was from the lowest to the largest flows, played a crucial role in determining how much sediment was available to be re-worked. At the 2% slope, the Q_1 flow did almost the same amount of work as the Q_{10} flow (0.042 and 0.044 m^3 of combined aggradation and degradation, respectively), but this is likely a function of the order the flows were conducted. The Q_{50} flow did the least amount of geomorphic work at the 2% slope, because there was very little mobile sediment remaining after the previous lower flows had deposited the available sediment in stable locations, thus potentially increasing the critical shear stress (Masteller et al., 2019). Therefore, examination of the cumulative geomorphic work for the successive flows is more appropriate within this experimental setup. The cumulative geomorphic work is naturally largest for the Q_{50} flow, as it has summed aggradation and degradation for previous flows; however, the cumulative geomorphic work for the Q_{50} flow is only approximately three times that of the Q_1 flow at the 2% flow. In channels with a broad or bimodal sediment distribution, clusters tend to remain stable unless the anchor sediment is entrained during high flows (Hendrick et al., 2010); therefore, once sediment clusters form at lower flows, those sediment particles are more difficult to mobilize even at higher flows.

At the 5% slope, the Q_1 and the Q_2 flows did similar amounts of geomorphic work, which was approximately three times the amount as that of the Q_{10} flow . This marked decrease in sediment transport during the Q_{10} flow can be explained in a similar way to that of the Q_{50} flow at the 2% slope, that all potentially mobile sediment had been mobilized and deposited in a stable setting before the Q_{10} flow. The Q_{50} flow did almost two and five times the amount of geomorphic work compared to the Q_2 and Q_{10} flows, respectively, at the 5% slope, but this is an artefact of slight downstream rotation of large clasts, which appears as downstream sedimentation and upstream degradation relative to boulders' previous positions. However, as these results are dependent on the sequencing of flows, they should not be interpreted as indicative of the relative amount of geomorphic work done by these flows over a longer period of time with a varying sequence of flow events. Had the higher flows preceded low flows, then the geomorphic work done by the lower flows would likely have been much lower. That said, these results can indicate whether the larger flows are capable of resetting the channel by reworking most of the bed sediment and entraining boulders. Because the Q_{50} flow did less geomorphic work than the Q_1 at the 2% slope, the Q_{50} is clearly not capable of reworking the channel bed. Although the Q_{50} flow did do more geomorphic work than the Q_1 flow at the 5% slope, the higher amount of work is an artefact of slight rolling of large clasts and thus the Q_{50} did not rework the channel bed at the higher slope either.

Through this flume experiment, it was only possible to test flows up to Q_{50}, due to the capacity of the pump; however, we can get a sense of the magnitude of flows necessary to transport boulders and re-work the channel bed. In this experiment, the geomorphic work done by the Q_{50} flow may be underestimated because it was preceded by several runs with lower flows that can cause interlocking of grains, thus increasing the necessary critical dimensionless shear stress (Masteller et al., 2019). However, given that the Q_{50} flow did not re-work the channel more than the Q_1 flow and no clasts >D_{84} were transported, we can conclude that the Q_{50} flow is not capable of disrupting grain interlocking in these channel types. In other steep, coarse-grained channels, boulder or bedform reorganization occurs during much lower recurrence interval flows; for example, step-pool structures in the Erlenbach, a small step-pool stream in Switzerland (18% slope), were completely rearranged three times within a 20-year period (Turowski et al., 2009). The recurrence intervals of the effective or channel-forming discharge in other steep coarse-bed channels have ranged from the Q_1 to the Q_{50} flow depending on slope, sediment size distribution and bedforms (Bunte et al., 2014; Hassan et al., 2014; Lenzi et al. 2006a), in addition to the local hydroclimatic regime controlling the magnitude of high recurrence-interval flows. Results from this study indicate that these semi-alluvial rapids in northern Sweden are similar to step-pool channels in alluvial, snowmelt-dominated Rocky Mountain streams where low flows may do a large amount of geomorphic work, depending on the history of previous flows (Bunte et al., 2014; Hassan et al., 2014). However, these low flows may only reflect a channel-maintaining and not a channel-forming flow (Hassan et al., 2014).

That begs the question of if fairly high flows (Q_{50}) are not capable of mobilizing boulders, what is the channel-forming flow and how did these channels originally form? Because of the snowmelt-dominated flow regime with buffering of flows by mainstem lakes, extremely high flows are unlikely (Arp et al., 2006; Bergstrand et al., 2014). The Q_{50} flow is only 1.8 times that of the Q_2 flow in this experiment, and the ratio of the Q_{50} to the Q_1 in this region ranges from 1.5-1.9 (Bergstrand et al., 2014). If the Q_{100} and Q_{500} flows follow the same logarithmic trend, those flows will only be 1.12 and 1.38 times that of the Q_{50} flow, respectively. Furthermore, the prototype channels are located in partly confined to unconfined moraine-, drumlin-, or esker-bounded floodplains, so flow depths would not increase significantly with higher flows. There are few mechanisms for post-glacial extreme flows in streams originating below the Scandes mountains in inland northern Sweden. Potential mechanisms for extreme flows, which do not follow the modeled RI-Q relationships, that cannot be ruled out include local cumulative effects of breached beaver dams or moraine-dammed lakes combined with a rain-on-snow event over seasonally-frozen ground. Based on the low magnitude of high-recurrence interval hydrologic events in this region, combined with results from this study showing that the Q_{50} flow is not channel-forming, it is unclear how often channel-forming flows, that are capable of transporting boulders, occur in these streams.

Large rivers in northern Sweden (e.g., Ume, Vindel, Lule Rivers) with steep bedrock gorges, to which these semi-alluvial channels are tributaries, were formed by sub-glacial meltwater while glaciers were melting ca 10,000 y. BP and have experienced very little fluvial erosion post-glaciation (Jansen et al., 2014). Although this study did not model higher than Q_{50} flows, there is a possibility that these semi-alluvial channels have not experienced a channel-forming discharge (capable of transporting boulders) since directly pre- or post-deglaciation when flow magnitudes could have been much larger and under higher pressure (Herman et al., 2011) and thus competent enough to move large boulders. Dimensionless shear stresses for D_{50} grains range from 0.009-0.027 at the 2% slope and 0.024-0.058 at the 5% slope (Table 2), which are well below critical dimensionless shear stress values of 0.056 for 2% slopes and 0.071 for 5% slopes (*sensu* Lamb et al. 2008). Given the non-linear increase in τ^*_c for larger grain sizes due to protrusion effects (e.g., Ashworth & Ferguson, 1989), the dimensionless shear stress values are not provided for D_{84} sediment, but can be assumed to be higher than the D50 lower than with a linear increase. Assuming Lamb et al.'s (2008) slope-dependent τ_c*-values, a flow depth of 0.14 m (1.8 times that of the Q_{50} flow depth) would be required just to entrain D_{50} sediment in the flume at the 2% slope; at the 5% slope, a water depth of 0.07 m (1.1 times that of the Q_{50} flow depth) flow would be required. If a τ_c*-value of 0.1 is assumed, which may be more appropriate in low RS-settings (Lenzi et al., 2006b), then depths of 0.25 m and 0.10 m are required at the 2% and 5% slopes, respectively. Due to the mostly unconfined to partly confined nature of the prototype streams, reaching analogous mean flow depths (1.1-2.0m and 0.57-0.81 m, respectively) would require very high magnitude flows to mobilize D_{50} sediment, let alone D_{84}-sized boulders. However, during deglaciation (~9000-10000 y BP), glaciers receded very rapidly at ~100 km in 100 years in the inland region below the Scandes mountains (Lundqvist, 1986; Stroeven et al., 2016), with the rate varying between 200 and 1600 m yr^{-1} in the region (Stroeven et al., 2016). This high deglaciation rate led to locally high discharges: modelled summer discharges in sub-glacial tunnels at the ice margin during deglaciation range from 100 to 300 m^3/s (Arnold & Sharp, 2002; Boulton et al., 2009). These post-glacial discharges are two orders of magnitude greater than the current Q_{50} and the extrapolated Q_{100} or Q_{500} flows and would thus be capable of transporting much larger clasts than current flow regimes allow. Since then, with the current snowmelt-dominated flow regime buffered by lakes, hydraulic processes provide few mechanisms for these channels to re-organize in terms of steps, pools or other large bedforms.

Another potential mechanism for localized sediment transport, including that of boulders, is winter ice cover and ice break-up (Lotsari et al., 2015; Polvi et al. 2020). Although boulders up to 2 m in diameter can be transported by ice during ice break-up (Lotsari et al., 2015), it is unclear how important the role of sporadic, localized transport by ice is for long-term channel formation (Ettema & Kempema, 2013). Therefore, channels may have inherited their overall geometry from unsorted glacial sediment, yet fluvial flows and ice processes from the current flow regime have likely promoted the formation of sediment clusters and control microhabitat formation.

4.2 Bedforms and sediment clusters

Within the flows modelled in this flume experiment, no classic alluvial steep-channel bedforms, such as step-pools, developed. Large clasts are not even transported by the Q_{50} flow, although some rotation and imbrication occurred at the highest flows. Thus the large clasts create fixed constrictions that the remainder of mobile sediment and potential instream wood and log jams form around. Even channel morphologies of steep alluvial channels (plane bed, step-pool, and cascades) are most likely controlled by the location of lateral constrictions and coarse sediments (Vianello & D'Agostino, 2007), and flow convergence at channel constrictions in pool-riffle channels play a major role in sediment routing and backwater development (Thompson & Wohl, 2009). Therefore, it is not surprising that immobile boulders would play a large role in the organization of the entire channel morphology. Thus neither Montgomery & Buffington's (1997) or Palucis & Lamb's (2017) general patterns regarding correlations between bedforms and slope apply in this environment. According to Montgomery & Buffington's (1997) bedform scheme, step-pools form in supply-limited systems. However, the setting for the prototype streams are severely transport-limited system due to the non-flashy hydrological regime, where very high magnitude flows are limited due to mainstem lakes and the unconfined valley geometries. Furthermore, channel widths may be too large to promote boulder jamming and thus step formation (Zimmerman et al., 2010).

Although no channel-spanning bedforms developed, there were patterns of sediment deposition and scour in relation to large clasts. These patterns are in accordance with previous studies on boulder-bed channels with low relative submergence regimes, where sediment will deposit upstream of large immobile boulders (Monsalve & Yager, 2017; Papanicolaou et al., 2011, 2018). However, in this study, this pattern was only observed at the highest flows (Q_{10} and Q_{50}) when large clasts were fully submerged but still with very low RS values (1-1.3). At lower flows (Q_1 and Q_2) where large clasts protruded above the water surface elevation and fully turbulent and hydraulically rough flows had not developed, more sediment deposited downstream of large clasts. After the Q_{10} and Q_{50} flows at both slope setups, sediment clusters of fine- to medium- sized sediment (D_{10} and D_{50}) formed upstream of large clasts. Previous flume experiments have examined the role of individual boulders on sediment deposition and have measured the hydraulics around large clasts in low RS, in terms of velocity, shear stress, and shear stress divergence. Monsalve and Yager (2017) observed sediment deposition upstream of large clasts and scour between clasts, which they explained formed as a result of negative bed shear stress divergence within a medium range of shear stress magnitudes so that size-selective entrainment is possible, in addition to the direction of bed shear stress vectors. Papanicolaou et al. (2018) note that the reversal in depositional locations in high RS versus low RS environments can be due to differences in the turbulent vortex structures and that the area or length of these structures relative to clasts may affect depositional areas. Furthermore, at low RS, the Froude number determines the location of sediment deposition: at subcritical flows, sediment deposits in the stoss of boulders but at supercritical flows, sediment can deposit at the upstream flanks of boulders (Papanicolaou et al., 2018). This pattern of upstream flank depositional zones was also observed in this study at the Q_{10} flow at the 5% slope, where local areas of supercritical flow with small hydraulic jumps were observed.

These previous flume studies of the effects of boulders in low RS regimes provide valuable insights into hydraulics and mechanisms of sediment deposition around boulders in low RS streams (e.g., Monsalve & Yager, 2017; Papanicolaou et al. 2011, 2018); however, in order to isolate the effects of individual boulders, these experiments represented oversimplified conditions than those found in the field in terms of boulder spacing and sediment size distribution. This study adds several layers of complexity that more accurately reflects field conditions of semi-alluvial channels by using a scaled down sediment distribution from field conditions of a prototype stream (Figure 4f), rather than a bimodal bed vs. boulder sediment distribution. Also, in contrast to previous studies where simple bed configurations were used, with isolated flow regimes where wakes do not interfere with those of consecutive boulders, boulders in this study were randomly located throughout the channel. Therefore, the data showed a large range in mean aggradation/degradation upstream and downstream of large clasts, as the stoss or lee side of one clast may be experiencing the effects of a proximal boulder located upstream, downstream or even laterally. Although a more controlled study can yield interesting data on hydraulic effects of single boulders, this study provides results that reflect the complexity and variability in field conditions. Therefore, even with large variation, statistically significant differences in the amount erosion/deposition around boulders can provide general trends of sediment patterns around boulders. Future work should expand on the detailed hydraulic measurements around boulders where large clasts are unevenly spaced, affecting one another, and have a wider grain size distribution, in order to determine the length and area of turbulent vortex structures around clasts (per Papanicolaou et al., 2018) and how they interact with one another to determine the areas of sediment deposition relative to large clasts.

The protrusion of large boulders can play an important role in determining potential sediment transport (Yager et al., 2007, 2012). Yager et al. (2007) found that protrusion of immobile grains determines the shear stress available to transport mobile sediment. Furthermore, protrusion decreases when sediment is deposited which in turn increases velocities and shear stress available to transport sediment. There is insufficient data in this experiment to determine whether there was a feedback in degree of protrusion, aggradation, and potential for further sediment transport. However, smoothing of the longitudinal profile, visualized through increased elevations upstream and downstream of protrusions suggest a decrease in protrusion (Figure S5).

4.3 Importance & widespread distribution of semi-alluvial channels

Recently, the importance of large grains in controlling processes in coarse-bed streams has gained prominence in the scientific literature (e.g., Williams et al., 2019). For example, MacKenzie and Eaton (2017) found that a slight increase in the D_{90} of a sediment size distribution caused a four-fold decrease in sediment transport. Rather than relying on the classic median grain size to determine sediment transport processes and channel morphology, MacKenzie et al. (2018) encourage us to examine the mobility of the largest grains in order to understand channel morphology. Similarly, Yager et al. (2018) argue that grain resistance, in particular that of large boulders that protrude from the channel, serve to increase the dimensionless critical shear stress so that the sediment transport threshold varies substantially among streams. Given these insights into the role of large grains in shaping sediment transport processes and thus channel morphology, semi-alluvial channels with abundant boulders relative to their transport capacity may form quite unique morphologies compared to alluvial channels.

Previous work on semi-alluvial channels have focused nearly solely on those with a mix of alluvial and bedrock elements, with either the channel bank or bed composed of bedrock (Turowski, 2012). However, few studies have examined sediment organization in semi-alluvial channels where immobile sediment reduces potential sediment transport and encourages sediment cluster formation. As many fluvial geomorphic studies have been conducted in temperate zones, beyond the limit of continental glaciation, or in mountain environments that are usually supply-limited, the sediment transport literature has focused on alluvial channels. The widespread distribution of continental glaciation-related till at northern latitudes probably means that boulder-bed semi-alluvial channels may also be widespread. Systematic global mapping of these channel types is lacking; however, mapping of Canadian channel types suggest that semi-alluvial streams are common in large parts of the Canadian Shield (Ashmore & Church, 2001). Understanding these boulder-bed semi-alluvial channels bridges previous research on semi-alluvial bedrock channels or low-gradient channels cut into peat or lacustrine sediment with that of steep coarse-bed channels in young mountain ranges. Even in young mountain ranges, hillslope-derived blocks (>1 m) can slow the rate of channel incision (Shobe et al., 2016), and thus could also be described as semi-alluvial.

Furthermore, at northern latitudes, mainstem lakes are widespread (Messager et al., 2016). With the exception of studies on the effects of lakes on sediment size in Maine, U.S.A. (Snyder et al., 2012) and the effect of lakes on downstream hydraulic geometry in Idaho, U.S.A. (Arp et al., 2007), the effect of lakes on geomorphic channel dynamics is little studied. Mainstem lakes buffer downstream sediment transport and will decrease the fine sediment available to be re-worked in a semi-alluvial rapid reach (Arp et al., 2007; Synder et al., 2012). In Fennoscandia, this decrease in available fine sediment is exacerbated by the overall low sediment yield on the continental shield due to the crystalline bedrock, cold climate and generally low relief (Polvi et al. 2020). These conditions that lead to low sediment yields are also common in the boreal shield regions of Canada, and may translate to similar low sediment yield stream systems. Fine sediment can only be recruited from channel banks and local tributary junctions. This interpretation is supported by analyses of sediment yields in Canada that show that sediment yield increases disproportionately with drainage area because sediment is eroded directly from streambanks. This indicates that rivers are degrading and that streams are eroding through Quaternary deposits of glacial sediment (Church et al. 1999). In addition to streambank sediment, some prototype reaches produce additional fine sediment from pre- or interglacially highly weathered bedrock or boulders of Revsunds granite (*personal observation*; *personal communication*, Rolf Zale). If greater amounts of fine sediment (sand to medium gravel) were available, it is possible that different patterns of deposition in relation to boulders would result.

4.4 Implications for restoration

In the past two decades, semi-alluvial rapids have been targeted for restoration, with >100 million Euro being spent to improve trout and salmon habitat in Sweden and Finland (e.g., Gardeström et al., 2013); however, positive ecological results have been sparse (Nilsson et al., 2015). Restoration has included increasing geomorphic complexity by adding large boulders, in addition to opening side channels and removing small dams, followed by adding spawning gravel downstream of boulders. However, based on the results from this flume experiment, to ensure the longevity of spawning beds, spawning gravel should not always be placed in downstream wakes in channels with low relative submergence regimes. In contrast to alluvial channels, the channel will likely not re-organize the restored major bed elements such as coarse boulders. Therefore, there is a larger burden on restoration practitioners to restore these streams correctly, in terms of balancing erosion and deposition and creating appropriate microhabitats.

5 Conclusions

A flume experiment was designed to elucidate how semi-alluvial boulder-bed channels with a snowmelt-dominated flow regime evolve in terms of potential bedforms or sediment clusters. These channels have a coarse sediment distribution, resembling that of steep mountain streams, but previous field observations have suggested that these channels do not form bedforms found in coarse-bed alluvial channels (*sensu* Montgomery & Buffington, 1997). My results confirmed that even a 50-year flow event does not reorganize bed sediment to form regular bedforms. However, patterns in sediment deposition were found in relation to boulders (>D_{84}): at moderate to high flows (Q_{10}-Q_{50}), finer sediment is deposited upstream of boulders rather than in downstream wakes. Because the geomorphic work done by the Q_{50} flow, following a sequence of lower flows, is less than that of the annual high-flow event (Q_1), it shows that the Q_{50} flow would not be able to disrupt grain interlocking and thus re-organize bedforms or boulders. This finding places these boulder-bed semi-alluvial channels in a different category than mountain streams, where many step-pool channels re-organize steps every 10-50 years (e.g., Bunte et al., 2014; Turowski et al., 2009). These results lead to the conclusion that the channel geometry of these semi-alluvial channels do not reflect equilibrium conditions based on the current snowmelt-dominated flow regime and sediment regime. The results from this study, combined with low-magnitude high-recurrence flows, due to mainstem lakes that buffer high flows and unconfined channel geometry, and the history of extremely high post-glacial flows, suggest that few channel-forming flows have occurred post-glaciation. Channels may instead have inherited their geometry from unsorted glacial sediment that was deposited from glacial meltwater sub-glacially or downstream of melting glaciers ca. 9000-10000 y. B.P.

Acknowledgments

Digital elevation models of the flume bed after each flow are available at https://doi.org/10.5878/kz4r-6y69 (Polvi, 2020). Funding for this research was provided by a R&D-project grant for young research leaders to L.E. Polvi from the Swedish Research Council Formas. I wish to thank Ellen Wohl for facilitating access to Colorado State University's Engineering Research Center and helpful preparatory discussions. I also thank the staff at the CSU Engineering Research Center who provided invaluable support in preparing the flume and executing the experiments, in particular Jason Berg and Taylor Hogan. I would like to thank Andy Bankert for assisting in setting up and processing the SfM scans and Dylan Armstrong for setting up and processing the LiDAR scans. Finally, I would like to thank several volunteers who helped set up the flume and carry out the experiments: William Amponsah, Truxton Blazek, Margherita Righini, Daniel Scott, Katherine Lininger, and Susan Cundiff. Thank you to Gabrielle David who commented on an earlier draft of the manuscript. Finally, I thank Peter Ashmore, Rob Ferguson and an anonymous reviewer whose constructive comments have greatly improved the manuscript.

References

Agisoft LLC. (2014). St. Petersburg, Russia.

Andrews, E. D. (1980). Effective and bankfull discharges of streams in the Yampa River Basin, Colorado, and Wyoming. *Journal of Hydrology, 46*, 311–330.

Arnold, N., & Sharp, M. (2002). Flow variability in the Scandinavian ice sheet: modelling the coupling between ice sheet flow and hydrology. *Quaternary Science Reviews, 21*, 485-502. https://doi.org/10.1016/S0277-3791(01)00059-2

Arp, C. D., Gooseff, M. N., Baker, M. A., & Wurtsbaugh, W. (2006). Surface-water hydrodyanamics and regimes of a small mountain stream-lake ecosystem. *Journal of Hydrology, 329*, 500-513. https://doi.org/10.1016/j.jhydrol.2006.03.006

Arp, C. D., Schmidth, J. C., Baker, M. A., & Myers, A. K. (2007). Stream geomorphology in a mountain lake district: hydraulic geometry, sediment sources and sinks, and downstream lake effects. *Earth Surface Processes and Landforms, 32*, 525-543. https://doi.org/10.1002/esp.1421

Ashmore, P., & Church, M. (2001). The impact of climate change on rivers and river processes in Canada. *Geological Survey of Canada, Bulletin* 555, 58 pp.

Ashworth, P. J., & Ferguson, R. I. (1989). Size-selective entrainment of bed load in gravel bed streams. *Water Resources Research, 25*, 627-634.

Bathurst, J. C. (2002). At-a-site variation and minimum flow resistance for mountain rivers. *Journal of Hydrology, 269*, 11-26. https://doi.org/10.1016/S0022-1694(02)00191-9

Bergstrand, M., Asp, S-S., & Lindström, G. (2014). Nationwide hydrological statistics for Sweden with high resolution using the hydrogical model S-HYPE. Hydrology Research, 45, 349-356. https://doi.org/10.2166/nh.2013.010

Boulton, G. S., Hagdorn, M., Maillot, P. B., & Zatsepin, S. (2009). Drainage beneath ice sheets: groundwater-channel coupling, and the origin of esker systems from former ice sheets. *Quaternary Science Reviews, 28*, 621-638. https://doi.org/10.1016/j.quascirev.2008.05.009

Bray, D. I. (1979). Estimating average velocity in gravel-bed rivers. *Journal of the Hydraulics Division- ASCE, 105*, 1103-1122.

Brummer, C. J., & Montgomery, D. R. (2003). Influence of coarse lag formation on the mechanics of sediment pulse dispersion in a mountain stream, Squire Creek, North Cascades, Washington, United States. *Water Resources Research, 42*(7), W07412. https://doi.org/10.1029/2005WR004776

Bunte, K., Abt, S. R., Swingle, K. W., & Cenderelli, D.A. (2014). Effective discharge in Rocky Mountain headwater streams. *Journal of Hydrology, 519*, 2136-2147. http://dx.doi.org/10.1016/j.jhydrol.2014.09.080

Chin, A., & Wohl, E. (2005). Toward a theory for step pool in stream channels, *Progress in Physical Geography: Earth and Environment, 29*, 275–296. https://doi.org/10.1191/0309133305pp449ra

Church, M. (2006), Bed material transport and the morphology of alluvial river channels, *Annual Review of Earth and Planetary Sciences, 34*, 325-354. https://doi.org/10.1146/annurev.earth.33.092203.122721

Church, M., Ham, D., Hassan, M., & Slaymaker, O. (1999). Fluvial clastic sediment yield in Canada: scaled analysis. *Canadian Journal of Earth Sciences, 36*, 1267-1280.

Church M., & Zimmerman, A. (2007). Form and stability of step−pool channels: Research progress. *Water Resources Research*, 43, W03415. https://doi.org/10.1029/2006WR005037

Coulombe-Pontbriand, M., & LaPointe, M. (2004). Geomorphic controls, riffle substrate quality, and spawning site selection in two semi-alluvial salmon rivers in the Gaspé Peninsula, Canada. *River Research and Applications, 20*, 577-590. https://doi.org/10.1002/rra.768

Curran, J. C., & Wilcock, P. R. (2005), Characteristic dimensions of the step−pool configuration: An experimental study, *Water Resoures. Research, 41*, W02030, https://doi.org/10.1029/2004WR003568.

David, G. C. L., Wohl, E., Yochum, S. E. & Bledoe, B. P. (2011). Comparative analysis of bed resistance partitioning in high-gradient streams. *Water Resources Research, 47*, W07507. https://doi.org/10.1029/2010WR009540

Downs, P.W., Soar, P.J., & Taylor, A. (2016). The anatomy of effective discharge: the dynamics of coarse sediment transport revealed using continuous bedload monitoring in a gravel−bed river during a very wet year. Earth Surface Processes and Landforms, 41, 147-161. https://doi.org/10.1002/esp.3785

Emmett, W. W., & Wolman, M. G. (2001). Effective discharge and gravel-bed rivers. *Earth Surface Processes and Landforms, 26*, 1369-1380. https://doi.org/10.1002/esp.303

Ettema, R., & Kempema, E.W. (2013). Ice effects on sediment transport. In *River Ice Formation ED: Spyros, B. Pp.297-338. Published by the Committee on River Ice Processes and the Environment, Canadian Geophysical Union Hydrology Section, Edmonton, Alberta, Canada* *http://cripe.civil.ualberta.ca/*

ESRI (2017). ArcGIS Desktop: v. 10.5.1. Redlands, CA: Environmental Systems Research Institute.

Faustini , J. M., Kaufmann, P. R., Herlihy, A. T. (2009). Downstream variation in bankfull width of wadeable streams across the conterminous United States, *Geomorphology, 108*, 292-311.

Gardeström, J., Holmqvist, D., Polvi, L.E., & Nilsson, C. (2013). Demonstration restoration measures in tributaries of the Vindel River catchment. *Ecology and Society, 18*(3), 8. http://dx.doi.org/10.5751/ES-05609-180308

Gran, K.B., Finnegan, N., Johnson, A. L., Belmont, P., Wittkop, C., & Rittenour, T. 2013. Landscape evolution, valley excavation, and terrace development following abrupt postglacial base-level fall. *Geological Society of America Bulletin, 125*, 1851-1864. http://dx.doi.org/10.1130/B30772.1

Grant, G.E. 1997. Critical flow constrains flow hydraulics in mobile-bed streams: A new hypothesis. Water Resources Research, 33, 349-358. http://dx.doi.org/10.1029/96WR03134

Hassan, M. A., Brayshaw, D., Alila, Y., & Andrews, E. (2014). Effective discharge in small formerly glaciated mountain streams of British Columbia: limitations and implications. *Water Resources Research, 50*, 4440-4458. http://doi/10.1002/2013WR014529.

Hendrick, R. R., Ely, L. L, & Papanicolaou, A. N. (2010). The role of hydrologic processes and geomorphology on the morphology and evolution of sediment clusters in gravel-bed rivers. *Geomorphology, 114*, 483-496. http://doi/10.1016/j.geomorph.2009.07.018

Herman, F., Beaud, F., Champagnac, J-D., Lemieux, J-M., & Sternai, P. (2011). Glacial hydrology and erosion patterns: A mechanism for carving glacial valleys. *Earth and Planetary Science Letters, 310*(3), 498-508. http://doi/10.1016/j.epsl.2011.08.022

Hey, R. D. (1979). Flow resistance in gravel-bed rivers. Journal of the Hydraulics Division-*ASCE, 105*, 365-379.

Jansen, J. D., Codilean, A. T., Stroeven, A. P., Fabel, D., Hättestrand, C., Kleman, J., et al. (2014). Inner gorges cut by subglacial meltwater during Fennoscandian ice sheet decay. *Nature Communications 5*, 3815. https://doi/10.1038/ncomms4815

Johnson, J. P. L. 2016. Gravel threshold of motion: a state function of sediment transport disequilibrium? *Earth Surface Dynamics, 4*, 685-703. https://doi/10.5194/esurf-4-685-2016

Julien, P. Y. (2002). *River Mechanics*. Cambridge, UK: Cambridge University Press.

Lamb, M. P., Dietrich, W. E., & Venditti, J. D. (2008). Is the critical Shields stress for incipient sediment motion dependent on channel-bed slope? *Journal of Geophysical Research, 113*, F02008. https://doi:10.1029/2007JF000831

Laronne, J. B., Garcia, C., & Reid, I. (2001). Mobility of patch sediment in gravel bed streams: patch character and its implications for bedload. In M. Paul Mosley (Ed.), *Gravel-Bed Rivers V* (pp. 249-289), Wellington, New Zealand: New Zealand Hydrological Society Inc.

Leach, J. A., & Laudon, H. (2019). Headwater lakes and their influence on downstream discharge. *Limnology and Oceanography Letters, 4*, 105-112. https://doi.org/10.1002/lol2.10110

Lee, A. J., & Ferguson, R. I. 2002. Velocity and flow resistance in step-pool streams. Geomorphology, 46, 59-71. https://doi.org/10.1016/S0169-555X(02)00054-5

Lenzi, M. A. (2001), Step−pool evolution in the Rio Cordon, northeastern Italy. *Earth Surface Processes Landforms,* 26, 991–1008. https://doi.org/10.1002/esp.239

Lenzi, M. A., Mao, L., & Comiti, F. (2006a). Effective discharge for sediment transport in a mountain river: computational approaches and geomorphic effectiveness. *Journal of Hydrology, 325*, 257-276. https://doi/10.1016/j.jhydrol.2005.10.031

Lenzi, M. A., Mao, L., & Comiti, F. (2006b). When does bedload transport begin in steep boulder-bed streams? *Hydrological Processes, 20*, 3516-3533. https://doi/10.1002/hyp.6168

Leopold, L. B., & Maddock, T. (1953). The hydraulic geometry of stream channels and some physiographic characteristics. Geological Survey Professional Paper 252.

Lind, L., Alfredsen, K., Kuglerová, L., & Nilsson, C. (2016). Hydrological and thermal controls of ice formation in 25 boreal stream reaches. *Journal of Hydrology, 540*, 797–811. https://doi/10.1016/j.jhydrol.2016.06.053

Lindström, G., Pers, C. P., Rosberg, R., Strömqvist, J., & Arheimer, B. (2010). Development and test of the HYPE (Hydrological Predictions for the Environment) model – A water quality model for different spatial scales. *Hydrology Research, 41*(3-4), 295-319. https://doi.org/10.2166/nh.2010.007

Lotsari, E., Wang, Y.S., Kaartinen, H., Jaakola, A., Kukko, A., Vaaja, M., Hyyppa, H., Hyyppa, J., & Alho, P. (2015). Gravel transport by ice in a subarctic river from accurate laser scanning. *Geomorphology, 246*, 113-122. https://doi.org/10.1016/j.geomorph.2015.06.009

Lundqvist, J. (1986). Late Weichselian glaciation and deglaciation in Scandinavia. *Quaternary Science Reviews, 5*, 269-292.

Lvovich, M. I., Karasik, G. Y., Bratseva, N. L., Medvedeva, G. P., & Maleshko, A. V. (1991). Contemporary Intensity of the World Land Intracontinental Erosion. Moscos: USSR Academy of Sciences.

MacKenzie, L.G., & Eaton, B.C. (2017). Large grains matter: contrasting bed stability and morphodynamics during two nearly identical experiments. *Earth Surface Processes and Landforms, 42*, 1287-1295. https://10.1002/esp.4122

MacKenzie, L. G., Eaton, B. C., & Church, M. (2018). Breaking from the average: why large grains matter in gravel−bed streams. *Earth Surface Processes and Landforms, 43*, 3190-3196. https://doi.org/10.1002/esp.4465

Masteller, C. C., Finnegan, N. J., Turowski, J. M., Yager, E. M., & Rickenmann, D. (2019). History-dependent threshold for motion revealed by continuous bedload transport measurements in a steep mountain stream. *Geophysical Research Letters, 46*, 2583-2591. https://doi.org/ 10.1029/2018GL081325

Meshkova, L. V., Carling, P. A., & Buffin-Bélanger T. (2012). Nomenclature, Complexity, Semi-alluvial Channels and Sediment-flux-driven Bedrock Erosion, In M. Church, P. M. Biron, A. Roy (Eds.), *Gravel-bed Rivers: Processes, Tools, Environments, First Edition* (pp. 424-431). Chichester, UK: John Wiley & Sons, Ltd.

Messager M. L., Lehner B., Grill G., Nedeva I. and Schmitt O. (2016). Estimating the volume and age of water stored in global lakes using a geo-statistical approach. *Nature Communications, 7*, 13603. https://doi/10.1038/ncomms13603

Monsalve, A., & Yager, E. M. (2017). Bed surface adjustments to spatially variable flow in flow relative submergence regimes. *Water Resources Research, 53*, 9350-6367. https://doi.org/10.1002/2017WR020845

Montgomery, D. R. (1999). Process domains and the river continuum. *Journal of the American Water Resources Association, 35*(2), 397-410. https://doi/10.1111/j.1752-1688.1999.tb03598.x

Montgomery, D. R., & Buffington, J. M. (1997). Channel-reach morphology in mountain drainage basins. *Geological Society of America Bulletin, 109*(5), 596-611. https://doi/10.1130/0016-7606(1997)109<0596:CRMIMD>2.3.CO;2

Morgan, J. A., Brogan, D. J., & Nelson, P. A. (2017). Application of structure-from-motion photogrammetry in laboratory flumes. *Geomorphology*, *276*, 125-143. https://doi.org/10.1016/j.geomorph.2016.10.021

Nilsson, C., Lepori, F., Malmqvist, B., Törnlund, E., Hjerdt, N., Helfield, J.M., et al. (2005). Forecasting environmental responses to restoration of rivers used as log floatways: an interdisciplinary challenge. Ecosystems, 8, 779–800. https://doi.org/10.1007/s10021-005-0030-9

Nilsson, C., Polvi, L. E., Gardeström, J., Hasselquist, E. M., Lind, L., & Sarneel, J. M. (2015). Riparian and in-stream restoration of boreal streams and rivers: success or failure? *Ecohydrology, 8*(5), 753-764. https://doi.org/10.1002/eco.1480

Nitsche, M., Rickenmann, D., Kirchner, J. W., Turowski, J. M., & Badoux, A. (2012). Macroroughness and variations in reach-averaged flow resistance in steep mountain streams. *Water Resources Research, 48*, W12518. https://doi.org/10.1029/2012WR012091

Palucis, M.C., & Lamb, M.P. (2017). What controls channel form in steep mountain streams? *Geophysical Research Letters*, 44, 7245-7255. https://doi.org/10.1002/2017GL074198

Papanicolaou, A. N., Dermisis, D. C., & Elhakeem, M. (2011). Investigating the role of clasts on the movement of sand in gravel bed rivers. *Journal of Hydraulic Engineering, 137*(9), 871-884. https://doi.org/10.1061/(ASCE)HY.1943-7900.0000381

Papanicolaou, A. N., & Kramer, C. (2005). The role of relative submergence on cluster microtopography and bedload predictions in mountain streams. In G. Parker & M. H. Garcia (Eds.), *4th IAHR symposium on river coastal and estuarine morphodynamics RCEM 2005* (pp. 1083- 1086).Urbana, IL: Taylor and Francis.

Papanicolaou, A. N., Kramer, C. M., Tsakiris, A. G., Stoesser, T., Bomminayuni S., & Chen, Z. (2012). Effects of a fully submerged boulder within a boulder array on the mean and turbulent flow fields: implications to bedload transport. *Acta Geophysica, 60*(6), 1502-1546. https://doi/10.2478/s11600-012-0044-6

Papanicolaou, A.N., Tsakiris, A.G., Wyssmanm, M.A., & Kramer, C.M. (2018). Boulder array effects on bedload pulses and depositional patches. *Journal of Geophysical Research- Earth Surface,* 123, 2925–2953. https://doi/10.1029/2018JF004753

Phillips, C. B., & Jerolmack, D. J. (2016). Self-organization of river channels as a critical filter on climate signals. *Science 352*, 694-697. https://doi/10.1126/science.aad3348

Pike, L., Gaskin, S., & Ashmore, P. (2018). Flume tests on fluvial erosion mechanisms in till-bed channels. *Earth Surface Processes and Landforms, 43*, 259-270.

Polvi, L.E. (2020). Morphology of boulder-bed semi-alluvial channel beds: a flume study modelling streams in northern Fennoscandia. Swedish National Data Service. https://doi.org/10.5878/kz4r-6y69 (Polvi, 2020).

Polvi, L.E., Dietze, M., Lotsari, E., Turowski, J.M., & Lind, L. (2020). Seismic Monitoring of a Subarctic River: Seasonal Variations in Hydraulics, Sediment Transport, and Ice Dynamics. *Journal of Geophysical Research- Earth Surface*, 125, e2019JF005333. https://doi.org/10.1029/2019JF005333

Polvi, L. E., Nilsson, C., & Hasselquist, E. M. (2014). Potential and actual geomorphic complexity of restored headwater streams in northern Sweden. *Geomorphology, 210*, 98-118. https://doi/10.1016/j.geomorph.2013.12.025

Reid, I., Frostick, F.E., Layman, J.T. (1985). The incidence and nature of bedload transport during flood flows in coarse grained alluvial channels. *Earth Surface Processes and Landforms, 10*, 33–44

Reid, H. E., Brierley, G. J., Mcfarlane, K., Coleman, S. E., & Trowsdale, S. (2013). The role of landscape setting in minimizing hydrogeomorphic impacts of flow regulation. International Journal of Sediment Research 28, 149-161. https://doi.org/10.1016/S1001-6279(13)60027-X

Rosenfeld, J., Hogan, D., Palm, D., Lundquist, H., Nilsson, C., & Beechie, T. J. (2011). Contrasting Landscape Influences on Sediment Supply and Stream Restoration Priorities in Northern Fennoscandia (Sweden and Finland) and Coastal British Columbia. Environmental Management, 47(1), 28-39. https://doi.org/10.1007/s00267-010-9585-0

RStudio Team (2016). RStudio: Integrated Development for R, v. 1.1.383. Boston, MA: RStudio, Inc. http://www.rstudio.com/

Sear, D. (1996). Sediment transport processes in pool-riffle sequences. *Earth Surface Processes and Landforms*, 21, 241-262. https://doi/ 10.1002/(SICI)1096-9837(199603)21:3<241::AID-SP623>3.0.CO;2-1

Seppälä, M. (2005). Glacially sculptured landforms, In M. Seppälä (Ed.), *The Physical Geography of Fennoscandia* (pp 35- 57). New York: Oxford University Press.

Shobe, C.M., Tucker, G.E., & Anderson, R.S. (2016). Hillslope-derived blocks retard river incision. *Geophysical Res. Letters, 43*, 5070-5078. https://doi.org/ 10.1002/2016GL069262

SMHI (2015). Vattenwebb: S-HYPE model data. Retrieved from http://vattenwebb.smhi.se/

SMHI (2017). Swedish Meteorological and Hydrological Institute. Retrieved from http://www.smhi.se

Stroeven, A. P., Hättestrand, C., Kleman, J., Heyman, J., Fabel, D., Fredin, O., et al. (2016). Deglaciation of Fennoscandia. *Quaternary Science Reviews, 147*, 91-121. https://doi.org/10.1016/j.quascirev.2015.09.016

Snyder, N. P., Castele, M. R., & Wright, J. R. (2008). Bedload entrainment in low-gradient paraglacial coastal rivers of Maine, U.S.A.: implications for habitat restoration. *Geomorphology 103*, 430-446. https://doi/10.1016/j.geomorph.2008.07.013

Synder, N., Nesheim, A. O., Wilkins, B. C, & Edmonds, D. A. (2012). Predicting grain size in gravel-bedded rivers using digital elevation models: application to three Maine watersheds. Geological Society of America Bulletin. https://doi/10.1130/B30694.1

Thompson, D. (2008). The influence of lee sediment behind large bed elements on bedload transport rates in supply-limited channels. *Geomorphology, 99*, 420-432. https://doi/https://doi.org/10.1016/j.geomorph.2007.12.004

Thompson, D. M., & Wohl, E. E. (2009).The linkage between velocity patterns and sediment entrainment in a forced-pool and riffle unit. *Earth Surface Processes and Landforms, 34*, 177-192. https://doi/10.1002/esp.1698

Torizzo, M., & Pitlick, J. (2004). Magnitude-frequency of bed load transport in mountain streams in Colorado. *Journal of Hydrology, 290*, 137-151. https://doi/10.1016/j.hydrol.2003.12.001

Turowski, J. M. (2012). Semi-alluvial channels and sediment-flux-driven bedrock erosion. In M. Church, P. M. Biron, A. Roy (Eds.), *Gravel-bed Rivers: Processes, Tools, Environments, First Edition* (pp. 401-416). Chichester, UK: John Wiley & Sons, Ltd.

Turowski, J. M., Yager, E. M., Badoux, A., Rickenmann, D., & Molnar, P. (2009). The impact of exceptional events on erosion, bedload transport and channel stability in a step-pool channel. *Earth Surface Processes and Landforms, 34*, 1661-1673. https://doi.org/10.1002/esp.1855

Vianello, A., & D’Agostino, V. (2007). Bankfull width and morphological units in an alpine stream of the dolomites (northern Italy). *Geomorphology, 83*, 266-281. https://doi.org/10.1016/j.geomorph.2006.02.023

Walling, D. E., & Webb, B. W., (1983). Patterns of sediment yield. In K. J. Gregory (Ed.), *Background to Palaeohydrology* (pp. 69-100). Chichester, UK: Wiley.

Westoby, M. J., Brasington J., Glasser, N. F., Hambrey, M. J., & Reynolds, J. M. (2012). ‘Structure-from-Motion’ photogrammetry: a low-cost, effective tool for geoscience applications. Geomorphology, 179, 300-314. https://doi.org/10.1016/j.geomorph.2012.08.021

Wheaton, J. M., Brasington, J., Darby, S. E., & Sear, D. A. (2010). Accounting for uncertainty in DEMs from repeat topographic surveys: improved sediment budgets. *Earth Surface Processes and Landforms, 35*, 136-156. https://doi/10.1002/esp.1886

Whittaker, J. G., & Jaeggi, M. N. R. (1982). Origin of step−pool systems in mountain streams, *Journal of the Hydraulic Division, ASCE, 108*, 758–773.

Williams, R. D., Reid, H. E., & Brierley, G. J. (2019). Stuck at the bar: larger-than-average grain lag deposits and the spectrum of particle mobility. *Journal of Geophysical Research- Earth Surface, 124,* 2751-2756. https://doi.org/10.1029/2019JF005137

Wolman, M. G., & Miller, J. P. (1960). Magnitude and frequency of forces in geomorphic processes. *J. Geol., 68*, 54–74.

Yager, E. M., Kirchner, J. W., & Dietrich, W. E. (2007). Calculating bed load transport in steep boulder bed channels. *Water Resources Research, 43*, W07418. https://doi.org/10.1029/2006WR005432

Yager, E. M., Turowski, J. M., Rickenmann D., & McArdell, B. W. (2012). Sediment supply, grain protrusion, and bedload transport in mountain streams. *Geophysical Research Letters, 39*, L10402. https://doi.org/10.1029/2012GL051654

Yager, E. M., Schmeeckle, M. W., & Badoux, A. (2018). Resistance is not futile: grain resistance controls on observed critical shields stress variations. *Journal of Geophysical Research- Earth Surface, 123*, 3308-3322. https://doi.org/10.1029/2018JF004817

Zimmermann, A., & Church, M. (2001). Channel morphology, gradient profiles and bed stresses during flood in a step−pool channel. *Geomorphology, 40*, 311–327. https://doi.org/10.1016/S0169-555X(01)00057-5

Zimmermann, A., Church, M., & Hassan, M. A. (2010). Step-pool stability: testing the jammed state hypothesis. *Journal of Geophysical Research- Earth Surface, 115*, F02008. https://doi.org/10.1029/2009JF001365

Water Resources Research

Supporting Information for

Morphodynamics of boulder-bed semi-alluvial streams in northern Fennoscandia: a flume experiment to determine sediment self-organization

L.E. Polvi

Department of Ecology & Environmental Science, Umeå University, Umeå, 907 36 Sweden

Contents of this file

Figures S1 to S5

Introduction

The supporting information provides additional background on prototype streams and additional data from flume results of boulder-bed semi-alluvial streams in northern Fennoscandia. The purpose of the flume experiments were to analyze changes in morphodynamics, in particular in relation to boulders, defined here as >D84 (624 mm in prototype streams). Figure S1 shows the flood-frequency relationship in the prototype streams with fairly low discharges even at high recurrence interval flows. These data are combined from field data of low-flow and annual high-flows and from regional hydrological models. Figure S2 graphically shows cumulative geomorphic work and aggradation/degradation after each flow, based on data shown in Table 3. Figures S3 and S4 show a representative portion of the DoDs (DEMs of difference) following each flow for the 2% and 5% slopes, respectively. These were created from structure-from-motion (combined with LiDAR-based control points) based DEMs, where photographs were taken after each flow. Figure S5 shows the longitudinal profile of the centerline of the flume after each flow at the 2% and the 5% slopes. The data for the longitudinal profiles were taken from the DEMs, created as described above.

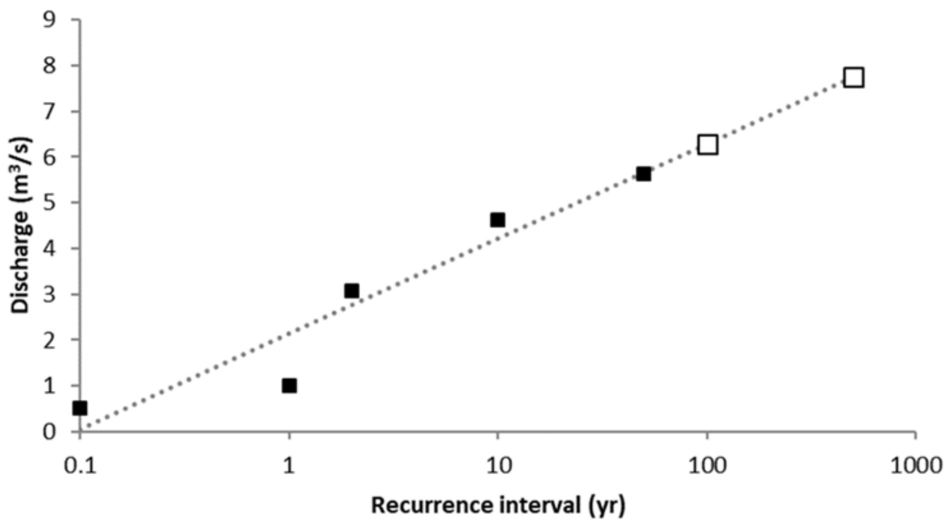

Figure S1. Flood frequency curve for prototype stream, calculated as average of nine streams. Flows for the recurrence interval of 0.1 and 1 years are from field data (Gardeström, unpublished data) and the flows with recurrence intervals of 2, 10 and 50 years are modeled using S-HYPE (Lindström et al., 2007; SMHI, 2015) (filled squares); the extrapolated values for the Q100 and Q500 flows based on the best-fit logarithmic line (dashed line) are shown as hollow squares.

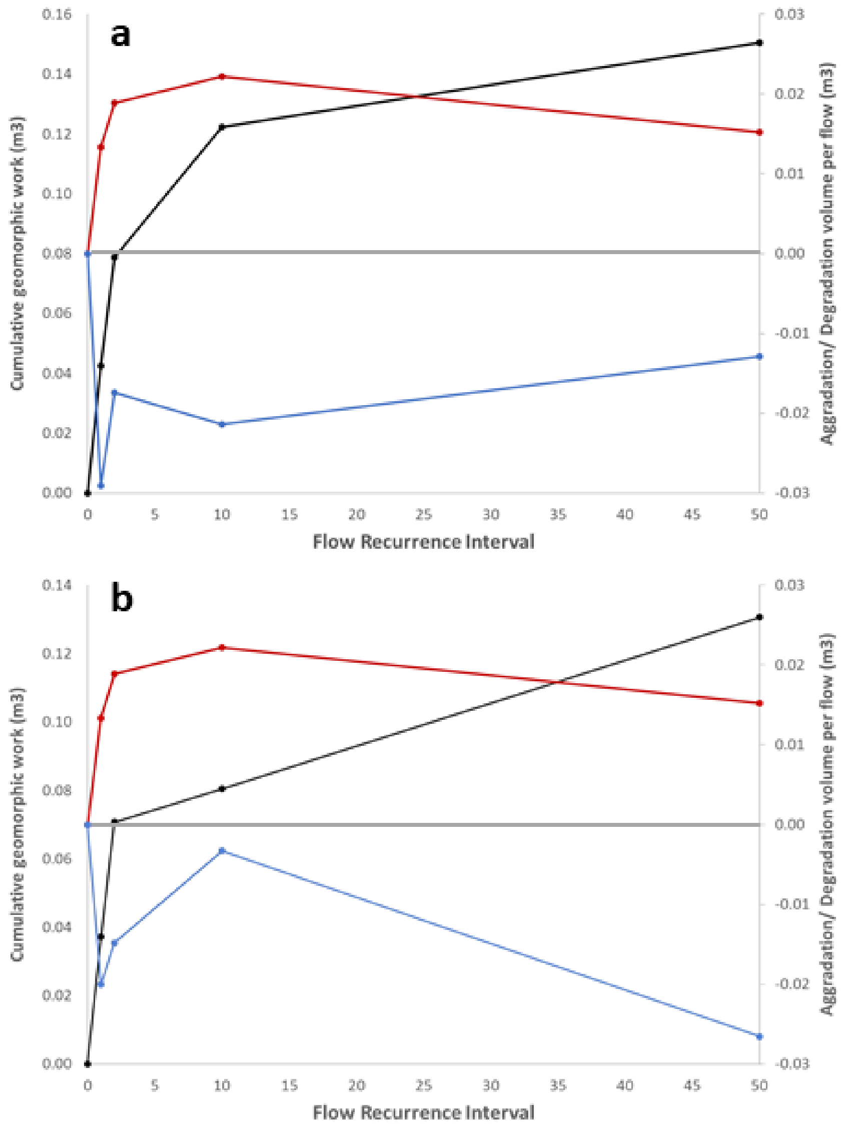

Figure S2. Cumulative geomorphic work (black line) for each of flows (Q1, Q2,Q10 & Q50), and aggradation (red line) and degradation (blue line) after each flow at (a) 2% slope and (b) 5% slope.

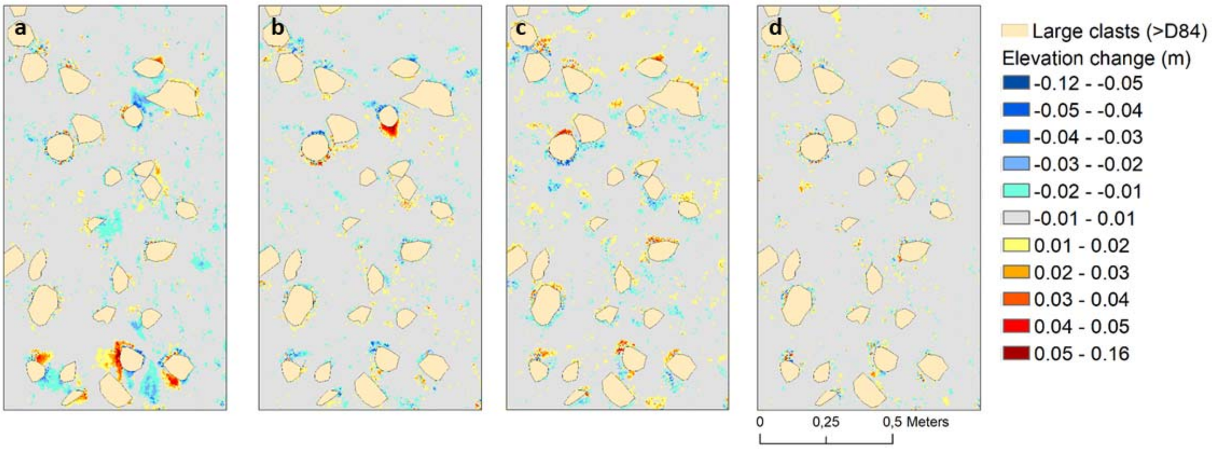

Figure S3. DEMs of difference after each flow at 2% slope compared to the previous flow, following the Q_1 flow (a), Q_2 flow (b), Q_{10} flow (c), and Q_{50} flow (d). Note that a representative portion of the flume is shown, rather than the entire flume, in order to aid in visualization and allow examination of patterns around large clasts.

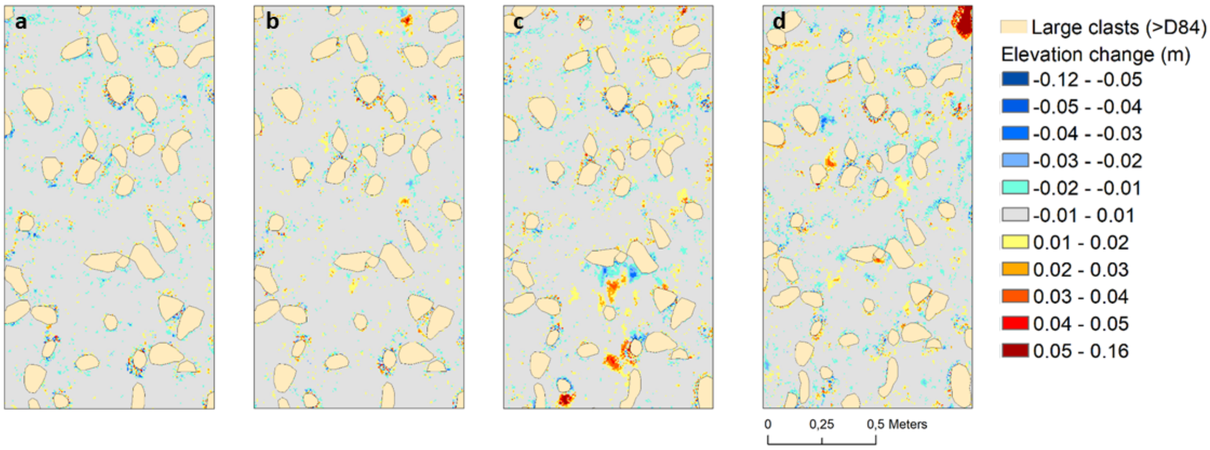

Figure S4. DEMs of difference after each flow at 5% slope compared to the previous flow, following the Q_1 flow (a), Q_2 flow (b), Q_{10} flow (c), and Q_{50} flow (d). Note that a representative portion of the flume is shown, rather than the entire flume, in order to aid in visualization and allow examination of patterns around large clasts.

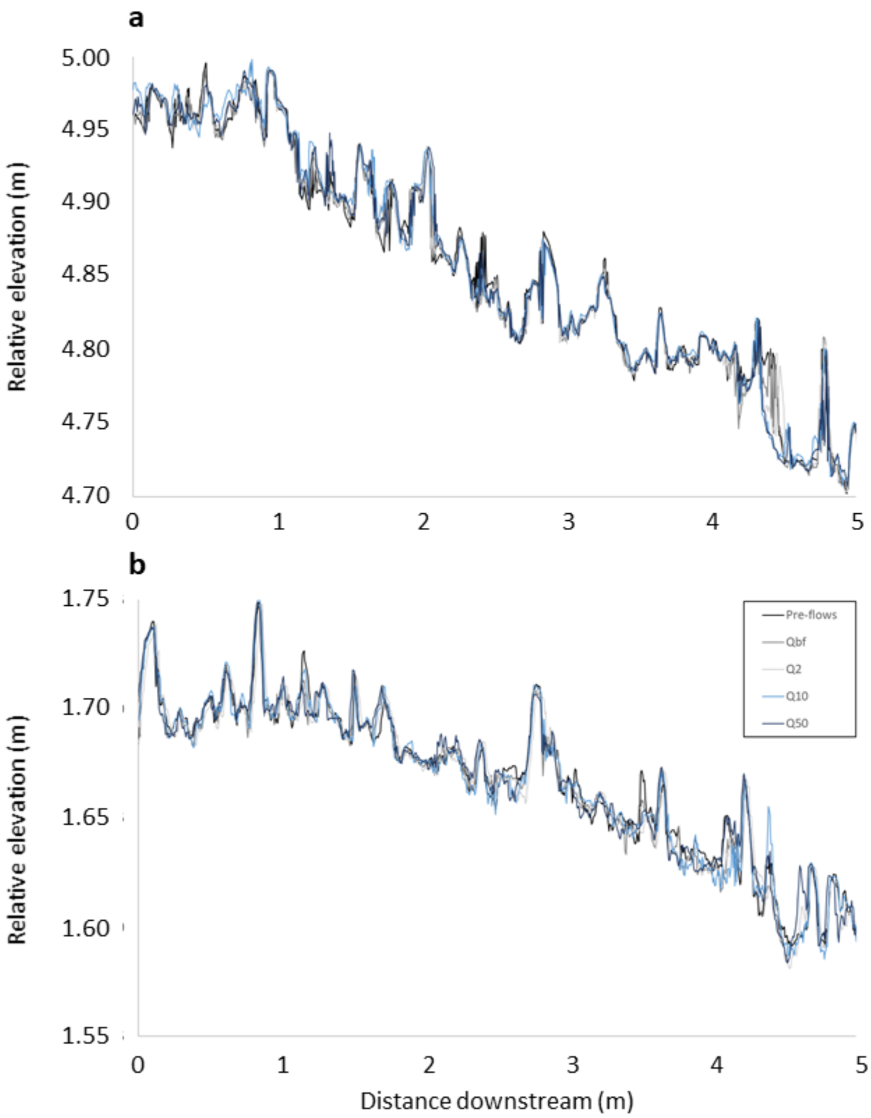

Figure S5. Longitudinal profiles of centerline in flume for initial conditions and following each subsequently higher flow for the 2% slope (a) and the 5% slope (b).